

Energy levels, radiative rates and electron impact excitation rates for transitions in Be-like Cl XIV, K XVI and Ge XXIX

Kanti M Aggarwal and Francis P Keenan

Astrophysics Research Centre, School of Mathematics and Physics, Queen's University Belfast, Belfast BT7 1NN, Northern Ireland, UK

e-mail: K.Aggarwal@qub.ac.uk

Received 31 July 2014

Accepted for publication 26 August 2014

Published xx Month 2014

Online at stacks.iop.org/PhysScr/vol/number

PACS Ref: 32.70 Cs, 34.80 Dp, 95.30 Ky

S This article has associated online supplementary data files

Tables 4–6 and 13–15 are available only in the electronic version at stacks.iop.org/PhysScr/vol/number

Abstract

Results for energy levels, radiative rates and electron impact excitation (effective) collision strengths for transitions in Be-like Cl XIV, K XVI and Ge XXIX are reported. For the calculations of energy levels and radiative rates the General-purpose Relativistic Atomic Structure Package (GRASP) is adopted, while for determining the collision strengths and subsequently the excitation rates, the Dirac Atomic R-matrix Code (DARC) is used. Oscillator strengths, radiative rates and line strengths are listed for all E1, E2, M1 and M2 transitions among the lowest 98 levels of the $n \leq 4$ configurations. Furthermore, lifetimes are provided for all levels and comparisons made with available theoretical and experimental results. Resonances in the collision strengths are resolved in a fine energy mesh and averaged over a Maxwellian velocity distribution to obtain the effective collision strengths. Results obtained are listed over a wide temperature range up to $10^{7.8}$ K, depending on the ion.

1 Introduction

Coronal lines of Be-like ions are useful for plasma diagnostics. In particular, the intensity ratio of the $2s^2 \ ^1S_0 - 2s2p \ ^3P_1^o$ and $2s2p \ ^1P_1^o - 2p^2 \ ^1D_2$ lines is temperature sensitive, as demonstrated by Landi *et al* [1] for a range of ions with $6 \leq Z \leq 28$. Similarly, the intensity ratio of the $2s2p \ ^3P_2^o - 2p^2 \ ^3P_2$ and $2s^2 \ ^1S_0 - 2s2p \ ^1P_1^o$ lines is density sensitive [2]. While these lines are in the UV range, the magnetic dipole ($2s2p$) $^3P_1^o - ^3P_2^o$ line of $17 \leq Z \leq 20$ lies in the visible [3]. In particular, lines of K XVI have been detected in solar spectra from the SERTS (solar EUV rocket telescope and spectrograph) rocket [4] as well as *Hinode* satellite [5]. Apart from astrophysical applications, Be-like ions are of interest in the modelling of fusion plasmas [6]. Several lines of Cl XIV and K XVI have been measured in laboratory plasmas by Huang *et al* [7]. Similarly, the $2s^2 \ ^1S_0 - 2s2p \ ^1P_1^o$ line of Ge XXIX at 92.8 \AA has been detected in the PLT (Princeton Large Torus) tokamak plasma by Stratton *et al* [8]. The importance of these ions has further increased with the developing ITER project. The ions which have been identified [9] for a greater interest are Al X, Cl XIV, K XVI, Ti XIX and Ge XXIX. Therefore, we have recently reported atomic data (i.e. energy levels, radiative rates and electron impact excitation rates) for Al X [10] and Ti XIX [11], and in this paper report similar results for Cl XIV, K XVI and Ge XXIX.

The experimental energy levels for these ions have been compiled and critically evaluated by the NIST (National Institute of Standards and Technology) team [12], and are available at the website <http://www.nist.gov/pml/data/asd.cfm>. Calculations for radiative rates (A- values) have been performed by many workers [13] – [17], but are restricted to the $n \leq 3$ levels. However, realising the importance of Be-like ions, many measurements have been made for their lifetimes, such as by [18]–[24]. These are helpful in assessing the accuracy of calculated A- values, as we will discuss in section 4. On the other hand, calculations for collision strengths (Ω) are very limited. For example, [13] and [25] calculated Ω for a wide range of Be-like ions with $8 \leq Z \leq 92$, but for a limited range of transitions within the $n = 3$ levels. Furthermore, unfortunately they did not report results for ions of Cl, K or Ge. However, Keenan [26] has provided analytical expressions, for transitions among the lowest 10 levels of the $n=2$ configurations, which allow the determination of effective collision strengths (Υ) for Cl XIV and K XVI, based on interpolation of R -matrix calculations for three Be-like ions, namely Ne VII, Si XI and Ca XVII. These results have been used in plasma modelling [2] and are stored in the CHIANTI [27] database at <http://www.chiantidatabase.org>. Since these data are not based on direct calculations for these ions, the available results can at best be described as preliminary, and hence there is scope for improvement as well as extension, as was the case with Al X [10]. Finally, for Ge XXIX the only calculations available in the literature for Ω are by [28], based on the *distorted-wave* (DW) method, which do not include the contribution of resonances. Also data for Ω are reported at only a single energy, and therefore the subsequent values of Υ may be significantly underestimated, because for Be-like ions the resonance structure is very dense, as demonstrated in our work on Ti XIX [11]. Therefore, here we report atomic data for energy levels, A- values, Ω and Υ for transitions among the lowest 98 levels of the $n \leq 4$ configurations of Cl XIV, K XVI and Ge XXIX.

As in most of our previous work, including on Be-like Al X [10] and Ti XIX [11], the fully relativistic GRASP (general-purpose relativistic atomic structure package) code has been used to calculate energy levels and A- values. Several versions of this code are available in the literature, but the one adopted here has been revised by one of the authors (Dr P H Norrington) and is freely available at the website <http://web.am.qub.ac.uk/DARC/>). This code is based on the jj coupling scheme, and apart from the one-body relativistic terms also includes corrections arising from the Breit interaction and QED effects (vacuum polarization and Lamb shift). Similarly, as in earlier research we have used the option of *extended average level* (EAL), in which a weighted (proportional to $2j+1$) trace of the Hamiltonian matrix is minimized. This produces a compromise set of orbitals describing closely lying states with moderate accuracy. For our calculations of Ω , we have adopted the *Dirac Atomic R-matrix Code* (DARC) of P H Norrington and I P Grant (<http://web.am.qub.ac.uk/DARC/>).

2 Energy levels

The 17 configurations of Be-like ions, namely $(1s^2) 2\ell 2\ell'$, $2\ell 3\ell$ and $2\ell 4\ell$, generate 98 levels. These are listed in Tables 1–3 for Cl XIV, K XVI and Ge XXIX, respectively. Also included in these tables are our level energies calculated from GRASP, *without* (GRASP1) and *with* (GRASP2) the contributions of the Breit and QED effects, as well as the values compiled by the NIST team [12]. However, NIST energies are restricted to the $n \leq 3$ levels and even then are not available for all levels, particularly in the case of Ge XXIX. As expected, the contributions of Breit and QED effects are negligible (≤ 0.04 Ryd) for Cl XIV and K XVI, but are slightly significant (up to 0.2 Ryd) for the comparatively heavy ion Ge XXIX – see for example, the $n = 4$ levels in Table 3. For a majority of levels, the energies have become lower with the inclusion of Breit and QED effects, but have increased for a few, particularly for $2s2p\ ^3P_0^o$.

Our energies obtained with the inclusion of the Breit and QED effects (GRASP2) are generally in good agreement (within 0.08 Ryd) with the NIST listings for most of the common levels. However, there are some exceptions. For example, for levels 5, 9 and 10 of Cl XIV, the NIST energies are lower by ~ 0.1 Ryd and higher by the same amount for level 27 ($2p3p\ ^3D_2$). Similar differences are noted for the same levels of K XVI, as found earlier for Al X [10] and Ti XIX [11]. Since NIST energies are not available for a majority of levels, the comparisons shown in Tables 1–3 are not very helpful for assessing the accuracy of our calculations. Therefore, also listed in these tables are the theoretical energies of Gu [29] for the lowest 10 levels and Safranova *et al* [30] for the higher ones, obtained from relativistic *many-body perturbation theory* (MBPT). In general, agreement between the GRASP and MBPT energies is highly satisfactory (within 0.1 Ryd) for a majority of levels and for all three ions. However, the MBPT energies are (mostly) closer to the NIST listings, although differences between the two are up to 0.1 Ryd (see for example, level 27 of Cl XIV in Table 1), i.e. the discrepancies are the same as with the GRASP calculations. We discuss these further.

Unpublished results of C Froese Fischer (2009), based on MCHF (multi-configuration Hartree-Fock) calculations are also available for 35 and 24 levels of Cl XIV and K XVI, respectively, on the website <http://nlte.nist.gov/MCHF/view.html>. Therefore, in table 1 we have included her results for Cl XIV for comparison. These energies are closer to the NIST listings and discrepancies, if any, are within 0.01 Ryd. Similarly, there is a good agreement between the MCHF and MBPT energies, and this clearly indicates that there is scope for improvement in our calculated energies with the GRASP code. This is further confirmed by the large-scale calculations of Cheng *et al* [31], based on relativistic configuration-interaction (RCI) method, who included over 200,000 configurations to determine energies of the lowest 4 levels of Be-like ions with $Z \leq 92$. As with the MBPT and MCHF calculations, their energies are in complete agreement, for all three ions under discussion here, with the experimental compilations of NIST. Finally, Jönsson *et al* [32] have demonstrated that the *convergence* in energy levels (and A- values), and a closer agreement with the experimental results, can be achieved for a range of ions, including Be-like, but with a very large expansion of configuration state functions (CSFs). For example, they included over 800,000 and 1,000,000 CSFs for the even and odd states of O IV to determine the $n \leq 3$ energy levels within 0.25% of the measurements. However, it must be stressed that such large calculations, although desirable, are not practically possible (particularly with the computational resources available with us) for a large number of levels, and especially when measurements are not available to compare with and to make accuracy assessment. Furthermore, the main focus in our work is on collisional data (discussed in sections 5 and 6) and for which a large set of CSFs cannot be included.

Since the comparisons of energies discussed above are restricted to the $n \leq 3$ levels and no prior results are available for the $n = 4$ levels, we have performed parallel calculations with the *Flexible Atomic Code* (FAC) of Gu [33], available from the website <http://sprg.ssl.berkeley.edu/~mfgu/fac/>. FAC, like GRASP, is also a fully relativistic code which provides a variety of atomic parameters, including energy levels. As shown in some of our earlier papers (see for example, [11] and [34]), results for energy levels and radiative rates obtained from FAC are comparable to those from GRASP. Hence calculations from FAC are helpful in assessing the accuracy of our energy levels, as well as radiative rates (which will be discussed in the next section). Therefore, listed in Tables 1–3 are results obtained from the FAC code (FAC1), which include the same CI

(configuration interaction) as in the GRASP calculations.

Our FAC1 level energies agree with our GRASP2 data within 0.05 Ryd for all levels and all ions. More importantly, the orderings are also the same. For some ions, a larger expansion of CI improves the accuracy of energy levels. To test this we have performed yet another calculation (FAC2), which includes a further 68 levels of the $2\ell 5\ell$ configurations. The FAC2 results are also included in Tables 1–3, but differences with the $n = 4$ calculations (FAC1) are negligible and the orderings of the levels are also the same. However, this (FAC2) expansion is insignificant in comparison to the large calculations [31]–[32] discussed above. Nevertheless, based on the comparisons discussed above we are confident that our energy levels listed in Tables 1–3 for Cl XIV, K XVI and Ge XXIX are accurate to better than 0.1 Ryd, or equivalently $\sim 2\%$. The accuracy of energy levels can be improved with the inclusions of *core-valence* and *core-core* correlations, apart from the *valence-valence* interactions included in our work. Similarly, orbitals of higher n will be helpful in improving the accuracy. Finally, we may state that all sets of energies, experimental and theoretical, agree within 0.1 Ryd and there is no discrepancy in their orderings, but scope remains for improving the accuracy of energy levels listed in tables 1–3.

3 Radiative rates

We have calculated A- values for four types of transition among the 98 levels, namely electric dipole (E1), electric quadrupole (E2), magnetic dipole (M1) and magnetic quadrupole (M2). Generally, A- values for E1 transitions dominate and hence are the most important. However, occasionally other types of transitions are also significant, such as (2s2p) $^3P_1^o - ^3P_2^o$ (M1), as mentioned in section 1. Therefore, for a complete plasma model, the inclusion of A- values for all types of transitions is generally preferable. In Tables 4–6 we list transition energies/wavelengths (λ , in Å), radiative rates (A_{ji} , in s^{-1}), oscillator strengths (f_{ij} , dimensionless), and line strengths (S , in a.u.), in length form only, for all 1468 electric dipole (E1) transitions among the 98 levels of Cl XIV, K XVI and Ge XXIX. The *indices* used to represent the lower and upper levels of a transition have already been defined in Tables 1–3. Similarly, there are 1754 electric quadrupole (E2), 1424 magnetic dipole (M1) and 1792 magnetic quadrupole (M2) transitions among the 98 levels. However, for these transitions only the A- values are listed in these tables, because the corresponding results for f- or S- values can be easily obtained using Eqs. (1–5) of [11]. Furthermore, the absorption oscillator strength (f_{ij}) and radiative rate A_{ji} (in s^{-1}) for all types of transitions are related by the following expression:

$$f_{ij} = \frac{mc}{8\pi^2 e^2} \lambda_{ji}^2 \frac{\omega_j}{\omega_i} A_{ji} = 1.49 \times 10^{-16} \lambda_{ji}^2 \frac{\omega_j}{\omega_i} A_{ji} \quad (1)$$

where m and e are the electron mass and charge, respectively, c is the velocity of light, λ_{ji} is the transition energy/wavelength in Å, and ω_i and ω_j are the statistical weights of the lower (i) and upper (j) levels, respectively.

Very limited data are available in the literature with which to compare our A- or f- values. Cheng *et al* [31] have reported A- values for 3 transitions of Be-like ions, namely 1–3 E1, 1–4 M2 and 1–5 E1, and their results agree within 10% with our calculations for all three ions. However, as for energy levels, unpublished results of C Froese Fischer (2009) are available on the website <http://nlte.nist.gov/MCHF/view.html> for 175 E1 transitions among the $n \leq 3$ levels of Cl XIV and K XVI. These calculations are based on her *multi-configuration Hartree-Fock* (MCHF) theory. Therefore, in Table 7 we compare our f- values with her data for both ions, but only for transitions from the lowest 5 levels. Also included in this table are the ratio (R) of the velocity and length forms (i.e. the Coulomb and Babushkin gauges in the relativistic terminology), because they give an indication of the accuracy of the calculations. As for the energy levels, agreement between the two sets of f- values is highly satisfactory and the discrepancies, if any, are under 20% for most transitions. There are slightly larger discrepancies (up to 50%) for some weak transitions, such as 3–12 ($f \sim 10^{-6}$) of Cl XIV. Similarly, for most transitions with significant f- values (> 0.01) R is within 20% of unity, although for a few weaker transitions (such as 5–6, $f \sim 10^{-5}$) the two forms of f- value differ considerably. Weak(er) transitions

are very sensitive to different levels of CI (and methods), because of the cancellation or addition of the mixing coefficients. Such large discrepancies are therefore common for almost all ions, with examples in both Al X [10] and Ti XIX [11].

The comparison of f- values discussed above is only for about 12% of the transitions, because of a paucity of other similar results. Therefore, as for energy levels, we have performed another calculation with the FAC code of Gu [33]. For all *three* ions the f- values from GRASP and FAC agree to within 20% for all strong transitions, as was also noted for other Be-like ions, see for example Table 3 for Al X [10] and Ti XIX [11]. Similarly, the effect of additional CI with the $n = 5$ configurations (166 levels in total) is negligible for most transitions of all ions. Therefore, based on the comparisons discussed above, and earlier ones for other Be-like ions, we may confidently state that the accuracy of our radiative data listed in Tables 4–6 is better than 20% for a majority of the (strong) transitions.

As for the E1 transitions, very limited data are available for comparison for other types of transition. In Table 8 we compare A- values for Cl XIV and K XVI for one M2 (1–4) and 11 M1 transitions with the MBPT calculations of Safronova [35] and Safronova *et al* [17]. Considering that most such transitions are very weak ($f \sim 10^{-6}$ or less), the agreement between the two sets of calculations is highly satisfactory, i.e. normally within 20%. Only for two transitions (7–9 and 8–9) are the discrepancies for both ions $\sim 50\%$. Overall, our listed A- values in Tables 4–6 for all types of transition are estimated to be accurate and reliable.

4 Lifetimes

The lifetime τ for a level j is defined as follows:

$$\tau_j = \frac{1}{\sum_i A_{ji}}. \quad (2)$$

Since several measurements for a few levels of Cl XIV and K XVI are available in the literature, in Tables 1–3 we have also listed our calculated lifetimes. Contributions from all four types of transitions, i.e. E1, E2, M1 and M2 are included for greater accuracy. In Table 9 we compare our calculated τ with measurements for the lowest 10 levels of Cl XIV. For all levels there are no discrepancies between theory and experiment, which confirms, yet again, the accuracy of our calculated A- values. Also included in this table are the MBPT results of Safronova *et al* [16] (and of Andersson *et al* [36] for level 5) which appear to be overestimated for the $2p^2$ $^3P_{0,1,2}$ levels by $\sim 50\%$, compared to measurements as well as with the present calculations. Finally, Träbert *et al* [24] measured τ for the $2s2p$ $^3P_2^o$ level of K XVI to be 7.6 ± 0.5 ms, and this compares very well with our result of 7.44 ms.

5 Collision strengths

The collision strength (Ω) and collision cross section (σ_{ij} , πa_0^2) are related by the following:

$$\Omega_{ij}(E) = k_i^2 \omega_i \sigma_{ij}(E) \quad (3)$$

where k_i^2 is the incident energy of the electron and ω_i is the statistical weight of the initial state. Results for collisional data are presented here in the form of Ω as it is a symmetric and dimensionless quantity.

The *Dirac atomic R-matrix code* (DARC), employed for the computation of collision strengths Ω , includes the relativistic effects in a systematic way, in both the target description and the scattering model. It is based on the jj coupling scheme, and uses the Dirac-Coulomb Hamiltonian in the *R*-matrix approach. The *R*-matrix radii adopted for Cl XIV, K XVI and Ge XXIX are 4.80, 4.40 and 2.40 au, respectively. For the expansion of the wavefunction, 55 continuum orbitals have been included for each channel angular momentum, which allow us to compute Ω up to energies of 660, 780 and 2500 Ryd for Cl XIV, K XVI and Ge XXIX, respectively. These energy ranges are sufficient to calculate values of effective collision strength Υ (see section 6) up to $T_e =$

$10^{7.8}$ K, well in excess of the temperature of maximum abundance in ionisation equilibrium for the ions under consideration [37]. The maximum number of channels for a partial wave is 428, and the corresponding size of the Hamiltonian matrix is 23 579. To obtain convergence of Ω , we have included all partial waves with angular momentum $J \leq 40.5$. This wide range of partial waves is sufficient for convergence of Ω for most transitions (particularly forbidden and inter-combination) and energies – see Figs. 1–3 of [11]. Furthermore, to account for higher neglected partial waves, we have included a top-up, based on the Coulomb-Bethe approximation [38] for allowed transitions and geometric series for others.

In Tables 10–12 we list our values of Ω for resonance transitions of Cl XIV, K XVI and Ge XXIX at energies *above* thresholds. The indices used to represent the levels of a transition have already been defined in Tables 1–3. Unfortunately, no similar data are available for comparison as already noted in section 1. As for energy levels and A- values, data for Ω can also be calculated with the FAC code. However, these data are not very useful for comparisons because there are often anomalies in the calculated Ω , as may be seen in Fig. 6 of [39]–[40]. Nevertheless, the qualitative agreement for most transitions in all three ions is similar to that already discussed for Al X [10] and Ti XIX [11].

6 Effective collision strengths

Excitation rates, as well as energy levels and A- values, are required for plasma modelling, and are determined from the collision strengths (Ω). Since the threshold energy region is dominated by numerous closed-channel (Feshbach) resonances, as shown in Figs. 6–11 of [11], values of Ω need to be calculated in a fine energy mesh so that their contribution can be included, which is often significant (if not dominant) particularly for forbidden and inter-combination transitions. Furthermore, for most (astrophysical and fusion) plasmas electrons have a wide distribution of velocities, and therefore values of Ω are averaged over a *Maxwellian* distribution as follows:

$$\Upsilon(T_e) = \int_0^\infty \Omega(E) \exp(-E_j/kT_e) d(E_j/kT_e), \quad (4)$$

where k is Boltzmann's constant, T_e electron temperature in K, and E_j the electron energy with respect to the final (excited) state. Once the value of Υ is known the corresponding results for the excitation $q(i,j)$ and de-excitation $q(j,i)$ rates can be easily obtained from the following equations:

$$q(i,j) = \frac{8.63 \times 10^{-6}}{\omega_i T_e^{1/2}} \Upsilon \exp(-E_{ij}/kT_e) \quad \text{cm}^3 \text{s}^{-1} \quad (5)$$

and

$$q(j,i) = \frac{8.63 \times 10^{-6}}{\omega_j T_e^{1/2}} \Upsilon \quad \text{cm}^3 \text{s}^{-1}, \quad (6)$$

where ω_i and ω_j are the statistical weights of the initial (i) and final (j) states, respectively, and E_{ij} is the transition energy. Values of Ω need to be determined over a wide energy range (above thresholds) to obtain convergence of the integral in Eq. (4), as clearly demonstrated in Fig. 7 of Aggarwal and Keenan [41].

To resolve resonances, we have performed our calculations of Ω at over $\sim 90\,660$ energies in the thresholds region, depending on the ion. Close to thresholds the energy mesh is 0.001 Ryd and is 0.002 Ryd elsewhere, particularly when the energy gap between two thresholds is rather wide – see for example levels 10 and 11 in Tables 1–3. Hence care has been taken to include as many resonances as possible, and with as fine a resolution as computationally feasible. The density and importance of resonances can be appreciated from Figs. 6–11 of [11]. For the present ions we observe similar resonances, but for brevity we show these in Figs. 1a–3a for only three transitions of Ge XXIX, namely 1–2 ($2s^2 \ ^1S_0 - 2s2p \ ^3P_0^o$), 1–4 ($2s^2 \ ^1S_0 - 2s2p \ ^3P_2^o$) and 2–3 ($2s2p \ ^3P_0^o - 2s2p \ ^3P_1^o$). Because of the large vertical scales of the figures the importance of the resonances appears to be insignificant, except for the 1–4 transition. Therefore, to appreciate their importance we make similar plots in Figs. 1b–3b, but with limited vertical scales. Although Ge XXIX is comparatively a heavy ion, resonances are

as dense, for all three transitions and many more, over the entire thresholds energy range as for lighter ions, and therefore make a significant contribution to Υ over a wide range of temperature.

Our calculated values of Υ are listed in Tables 13–15 over a wide temperature range up to $10^{7.8}$ K, suitable for applications to a variety of plasmas. As stated in section 1, the only available data for comparison are those of [26], which are obtained from the interpolation of R -matrix calculations for Ne VII, Si XI and Ca XVII. Therefore, in Tables 16 and 17 we compare our values of Υ with those of [26] for transitions among the lowest 10 levels, and at three temperatures of Cl XIV ($\log T_e = 6.3, 6.5$ and 6.7 K) and K XVI ($\log T_e = 6.5, 6.7$ and 6.9 K). Also included for easy guidance in these tables are the ratio of our and the Υ values of [26] at all three temperatures. As expected, agreement between the two sets of results for (most) allowed transitions is highly satisfactory for both ions – see for example, 1–5, 2–7 and 3–6 in Tables 16–17. However, for forbidden transitions, such as 1–6/7/8 ($2s^2 \ ^1S_0 - 2p^2 \ ^3P_{0,1,2}$) and 2–8/9/10 ($2s2p \ ^3P_0^o - (2p^2) \ ^3P_2, \ ^1D_2, \ ^1S_0$), the Υ of [26] are underestimated by up to a factor of 4. A similar effect of resonances (and/or discrepancy between two sets of Υ) was observed for transitions of Al X [10], and is fully expected considering the resonances observed in Figs. 1–3.

7 Conclusions

In this paper we have presented results for energy levels and radiative rates for four types of transitions (E1, E2, M1 and M2) among the lowest 98 levels of the $n \leq 4$ configurations for three Be-like ions, namely Cl XIV, K XVI and Ge XXIX. These ions are of interest for both astrophysical and fusion plasmas. Additionally, lifetimes of all the calculated levels have been reported, and these compare well with measurements. Therefore, based on this and a variety of other comparisons among various calculations, including analogous ones with the FAC code, our GRASP results for radiative rates, oscillator strengths, line strengths and lifetimes are assessed to be accurate to better than 20% for a majority of the strong transitions (levels). Similar comparisons for collision strengths are not possible due to a paucity of data in the literature. However, based on our experience with similar calculations for other Be-like ions, namely Al X [10] and Ti XIX [11], the accuracy of our values of Ω_s is $\sim 20\%$ for most transitions. For calculations of effective collision strength (Υ), resonances in the thresholds energy region are resolved in a fine energy mesh and are noted to be dominant for many transitions. Their contribution to the calculation of Υ is hence significant for all three ions of present interest. Furthermore, we have considered a large range of partial waves to achieve convergence of Ω at most energies and have adopted a wide energy range to calculate values of Υ up to $T_e = 10^{7.8}$ K. Therefore, we estimate the accuracy of our results for Υ to be better than 20% for most transitions. Earlier available interpolated results for Cl XIV and K XVI are found to be underestimated by up to a factor of four, particularly for the forbidden transitions. We believe the present set of complete results for radiative and excitation rates for transitions in CL XIV, K XVI and Ge XXIX will be useful for the modelling of a variety of plasmas, including astrophysical and fusion.

Acknowledgment

KMA is thankful to AWE Aldermaston for financial support.

References

- [1] Landi E, Doron R, Feldman U and Doschek G A 2001 *Astrophys. J.* **556** 912
- [2] Keenan F P, Boylan M B, Cheshire R C and Conlon E S 1991 *Phys. Scr.* **44** 351
- [3] Collins P D B 1964 *Astrophys. J.* **140** 1206
- [4] Thomas R J and Neupert W M 1994 *Astrophys. J. Suppl.* **91** 461
- [5] Del Zanna G 2008 *Astron. Astrophys.* **481** L69
- [6] Feldman U and Seely J F 1985 *At. Data Nucl. Data Tables* **32** 305
- [7] Huang L K, Lippmann S, Yu T L, Stratton B C, Moos H W, Finkenthal M, Hodge W L, Rowan W L, Richards B, Phillips P E and Bhatia A K 1987 *Phys. Rev. A* **35** 2919
- [8] Stratton B C, Moos H W, Suckewer S, Feldman U, Seely J F and Bhatia A K 1985 *Phys. Rev. A* **31** 2534
- [9] Rose S J 2012 private communication
- [10] Aggarwal K M and Keenan F P 2014 *Month. Not. R. astron. Soc.* **438** 1223
- [11] Aggarwal K M and Keenan F P 2012 *Phys. Scr.* **86** 055301
- [12] Kramida A,Ralchenko Y, Reader J and NIST ASD Team, 2013 NIST Atomic Spectra Database (version 5.1) Online at: <http://physics.nist.gov/asd>
- [13] Zhang H and Sampson D H 1992 *At. Data Nucl. Data Tables* **52** 143
- [14] Jönsson P, Froese Fischer C and Träbert E 1998 *J. Phys. B* **31** 3497
- [15] Safranova U I, Derevianko A, Safranova M S and Johnson W R 1999 *J. Phys. B* **32** 3527
- [16] Safranova U I, Johnson W R, Safranova M S and Derevianko A 1999 *Phys. Scr.* **59** 286
- [17] Safranova U I, Johnson W R and Derevianko A 1999 *Phys. Scr.* **60** 46
- [18] Ishii K, Alvarez E, Hallin R, Lindskog J, Marelius A, Pihl J, Sjödin R, Denne B, Engström L, Huldt S and Martinson I 1978 *Phys. Scr.* **18** 57
- [19] Forester J P, Pegg D J, Griffin P M, Alton G D, Elston S B, Hayden H C, Thoe R S, Vane C R and Wright J J 1978 *Phys. Rev. A* **18** 1476
- [20] Kawatsura K, Sataka A, Ootuka A, Komaki K, Naramoto H, Fujimoto F, Nakai Y and Ishii K 1987 *Nucl. Inst. Methods* **A262** 150
- [21] Sakata M, Ozawa K, Kawatsura K, Ootuka A, Komaki K, Naramoto H, Fujimoto F and Nakai Y 1988 *J. Phys. Soc. Japan* **57** 3352
- [22] Wouters A, Schwob J L, Suckewer S, Seely J F, Feldman U and Davé J H 1988 *J. Opt. Soc. Am. B* **5** 1520
- [23] Bhattacharya N, Bapat B, Rangwala S A, Kumar S V K and Krishnakumar E 1998 *Eur. Phys. J. D* **2** 125
- [24] Träbert E, Beiersdorfer P, Brown G V, Chen H, Pinnington E H and Thorn D B 2001 *Phys. Rev. A* **64** 034501
- [25] Sampson D H, Goett S J and Clark R E H 1984 *At. Data Nucl. Data Tables* **30** 125

- [26] Keenan F P 1988 *Phys. Scr.* **37** 57
- [27] Landi E, Young P R, Dere K P, Del Zanna G and Mason H E 2013 *Astrophys. J.* **763** 86
- [28] Bhatia A K 1986 *At. Data Nucl. Data Tables* **35** 449
- [29] Gu M F 2005 *At. Data Nucl. Data Tables* **89** 267
- [30] Safronova M S, Johnson W R and Safronova U I 1997 *J. Phys.* **B30** 2375
- [31] Cheng K T, Chen M H and Johnson W R 2008 *Phys. Rev. A* **77** 052504
- [32] Jönsson P, Godefroid G, Gaigalas G, Bieroń J and Brage T 2013 *Am. Inst. Phys. Proc.* **1545** 266
- [33] Gu M F 2008 *Can. J. Phys.* **86** 675
- [34] Aggarwal K M, Tayal V, Gupta G P and Keenan F P 2007 *At. Data Nucl. Data Tables* **93** 615
- [35] Safronova U I 2000 *Mol. Phys.* **98** 1213
- [36] Andersson M, Zou Y and Hutton R 2009 *Phys. Rev. A* **79** 032501
- [37] Bryans P, Landi E and Savin D W 2009 *Astrophys. J.* **691** 1540
- [38] Burgess A and Sheorey V B 1974 *J. Phys.* **B7** 2403
- [39] Aggarwal K M and Keenan F P 2012 *Phys. Scr.* **85** 025305
- [40] Aggarwal K M and Keenan F P 2012 *Phys. Scr.* **85** 025306
- [41] Aggarwal K M and Keenan F P 2008 *Eur. Phys. J. D* **46** 205

Fig. 1a. Collision strengths for the 1–2 transition of Ge XXIX

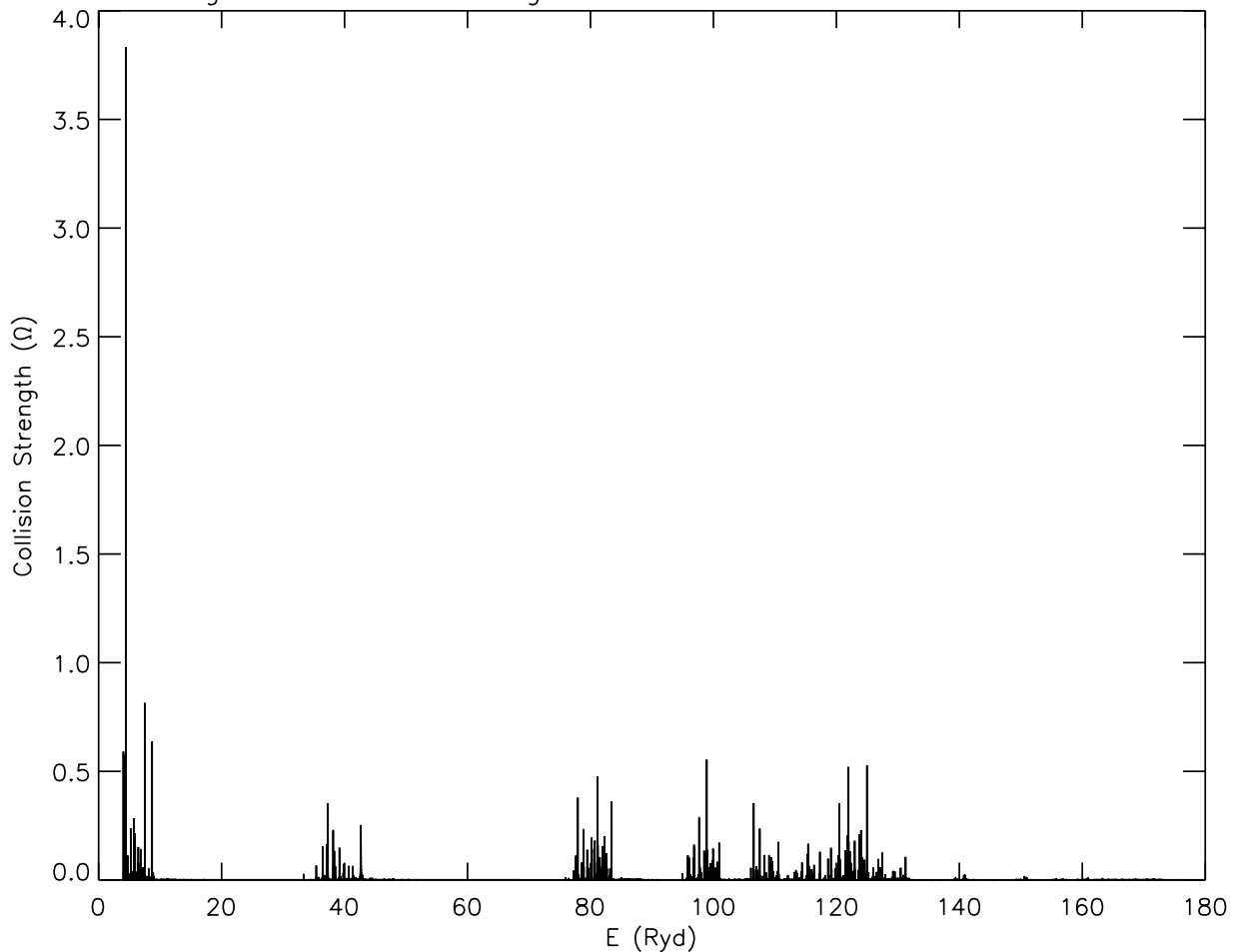


Figure 1: (a and b) Collision strengths for the $2s^2 \ ^1S_0 - 2s2p \ ^3P_0^o$ (1–2) transition of Ge XXIX.

Fig. 1b. Collision strengths for the 1–2 transition of Ge XXIX

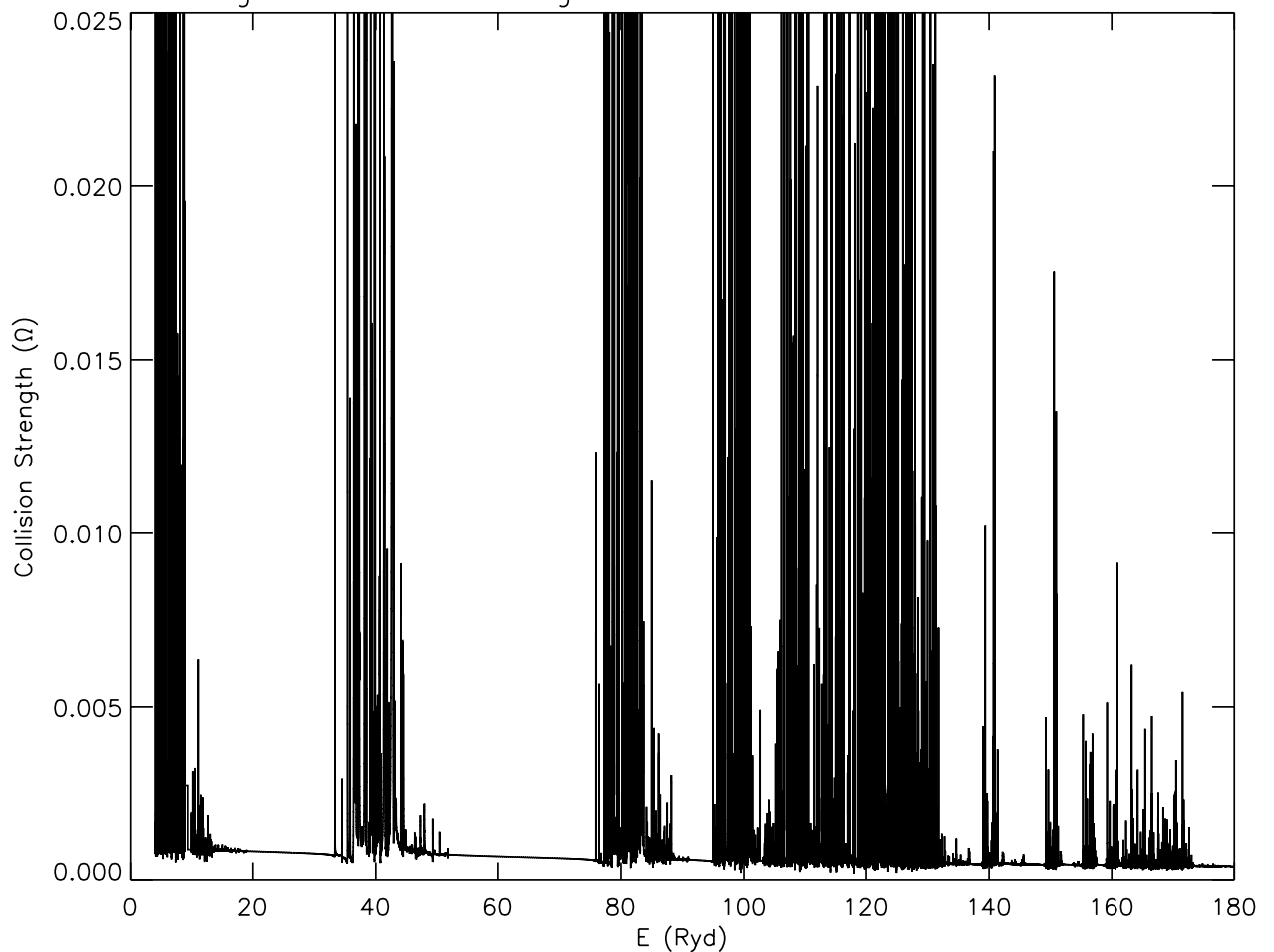


Figure 1: (a and b) Collision strengths for the $2s^2 \ ^1S_0 - 2s2p \ ^3P_0^o$ (1–2) transition of Ge XXIX.

Fig. 2a. Collision strengths for the 1–4 transition of Ge XXIX

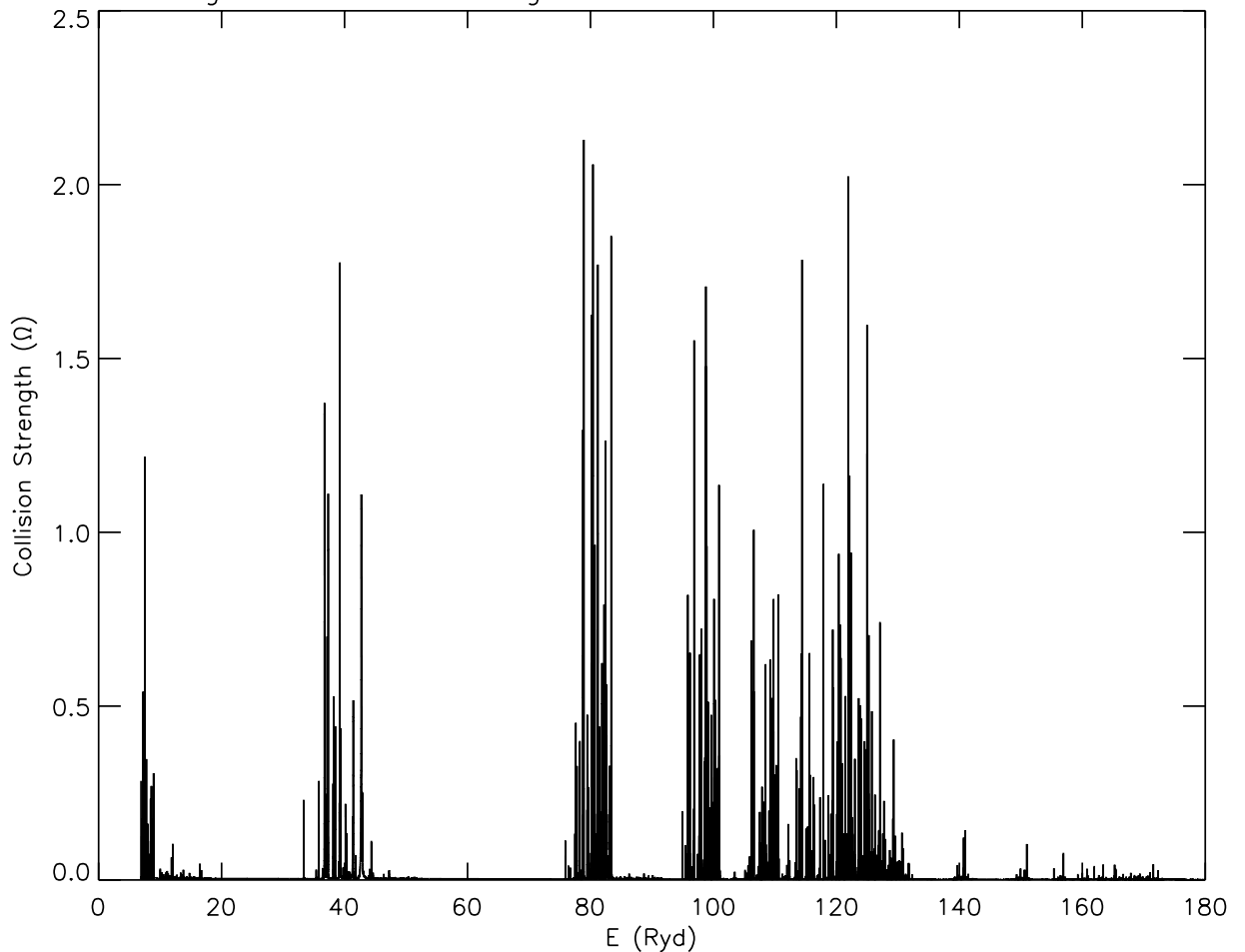


Figure 2: (a and b) Collision strengths for the $2s^2 \ ^1S_0 - 2s2p \ ^3P_2^o$ (1–4) transition of Ge XXIX.

Fig. 2b. Collision strengths for the 1–4 transition of Ge XXIX

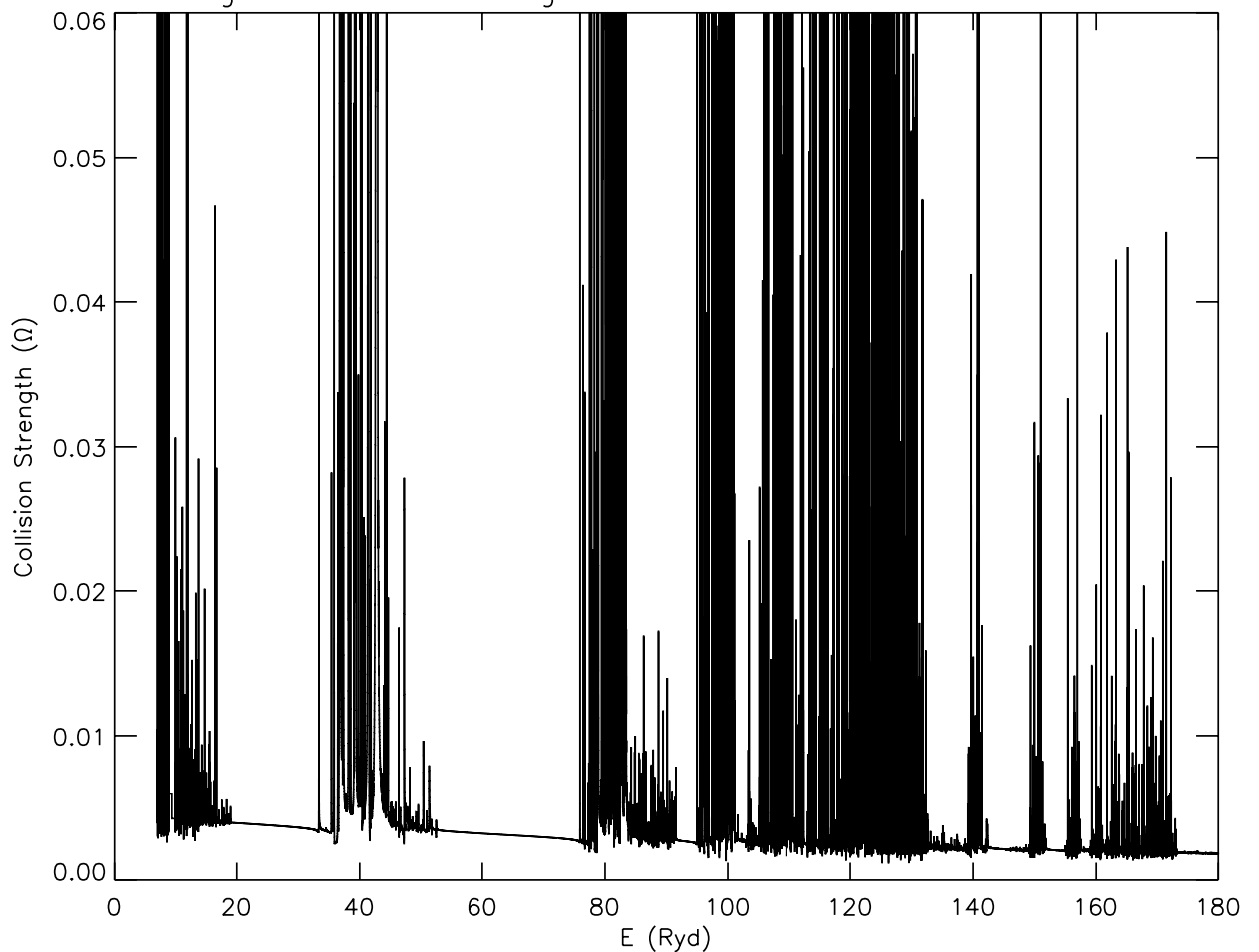


Figure 2: (a and b) Collision strengths for the $2s^2 \ ^1S_0 - 2s2p \ ^3P_2^o$ (1–4) transition of Ge XXIX.

Fig. 3a. Collision strengths for the 2–3 transition of Ge XXIX

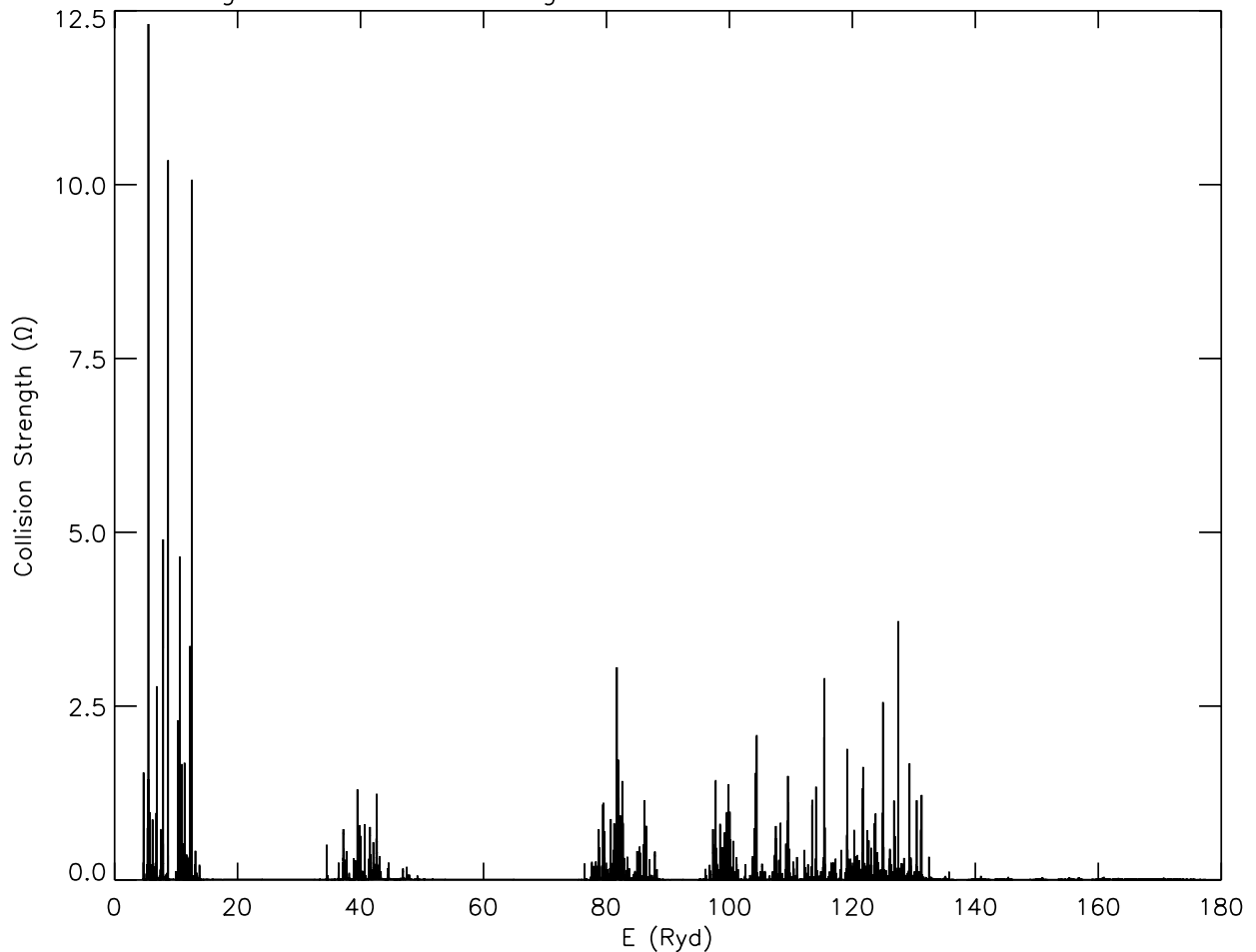


Figure 3: **(a and b)** Collision strengths for the $2\text{s}2\text{p } ^3\text{P}_0^o - 2\text{s}2\text{p } ^3\text{P}_1^o$ (2–3) transition of Ge XXIX.

Fig. 3b. Collision strengths for the 2–3 transition of Ge XXIX

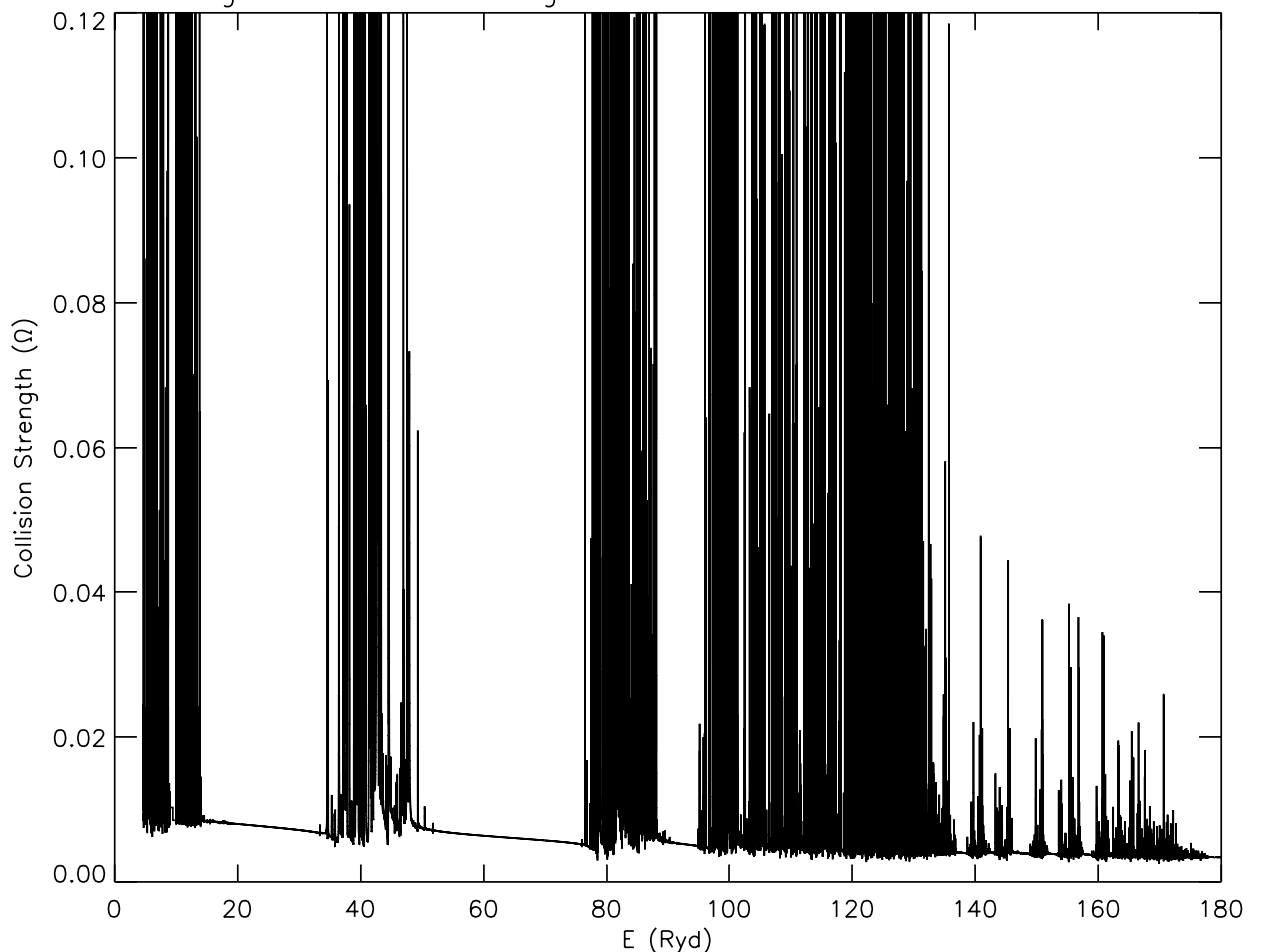


Figure 3: **(a and b)** Collision strengths for the $2s2p\ ^3P_0^o - 2s2p\ ^3P_1^o$ (2–3) transition of Ge XXIX.

Table 1: Energy levels (in Ryd) of Cl XIV and their lifetimes (τ , s). $a \pm b \equiv a \times 10^{\pm b}$.

Index	Configuration	Level	NIST	MBPT	MCHF	GRASP1	GRASP2	FAC1	FAC2	τ (s)
1	2s ²	¹ S ₀	0.0000	0.0000	0.0000	0.0000	0.0000	0.0000	0.0000
2	2s2p	³ P ₀ ^o	1.9493	1.9503	1.9481	1.9503	1.9546	1.9628	1.9622
3	2s2p	³ P ₁ ^o	2.0004	2.0014	1.9992	2.0064	2.0055	2.0134	2.0128	6.052-07
4	2s2p	³ P ₂ ^o	2.1179	2.1190	2.1167	2.1301	2.1222	2.1293	2.1288	3.464-02
5	2s2p	¹ P ₁ ^o	3.8319	3.8284	3.8356	3.9138	3.9108	3.9094	3.9046	1.102-10
6	2p ²	³ P ₀	5.1378	5.1388	5.1402	5.1706	5.1729	5.1908	5.1900	1.500-10
7	2p ²	³ P ₁	5.2068	5.2079	5.2078	5.2422	5.2408	5.2583	5.2575	1.449-10
8	2p ²	³ P ₂	5.3017	5.3032	5.3035	5.3476	5.3361	5.3528	5.3521	1.415-10
9	2p ²	¹ D ₂	5.8199	5.8158	5.8244	5.9064	5.8973	5.9130	5.9090	5.677-10
10	2p ²	¹ S ₀	7.1114	7.1076	7.1188	7.2461	7.2471	7.2556	7.2529	7.051-11
11	2s3s	³ S ₁	31.5180	31.5216	31.5240	31.5186	31.5033	31.5022	31.5019	1.584-12
12	2s3s	¹ S ₀		31.8883	31.8903	31.8868	31.8723	31.8854	31.8851	4.513-12
13	2s3p	¹ P ₁ ^o	32.4147	32.4084	32.4107	32.4174	32.4020	32.4130	32.4122	7.494-13
14	2s3p	³ P ₀ ^o			32.4345	32.4337	32.4204	32.4321	32.4323	1.122-10
15	2s3p	³ P ₁ ^o	32.4766	32.4594	32.4605	32.4643	32.4480	32.4591	32.4589	2.019-12
16	2s3p	³ P ₂ ^o			32.4815	32.4841	32.4674	32.4784	32.4785	9.567-11
17	2s3d	³ D ₁	32.9624		32.9635	32.9711	32.9528	32.9674	32.9652	2.960-13
18	2s3d	³ D ₂	32.9715	32.9685	32.9695	32.9780	32.9587	32.9732	32.9710	2.980-13
19	2s3d	³ D ₃	32.9778		32.9793	32.9885	32.9686	32.9829	32.9806	3.007-13
20	2s3d	¹ D ₂	33.3223	33.3151	33.3213	33.3611	33.3424	33.3559	33.3520	4.362-13
21	2p3s	³ P ₀ ^o			33.9707	33.9765	33.9640	33.9901	33.9903	2.066-12
22	2p3s	³ P ₁ ^o		34.0125	34.0143	34.0236	34.0086	34.0346	34.0347	2.005-12
23	2p3s	³ P ₂ ^o			34.1458	34.1613	34.1382	34.1629	34.1630	1.932-12
24	2p3s	¹ P ₁ ^o			34.4507	34.4974	34.4773	34.5086	34.5047	1.548-12
25	2p3p	¹ P ₁		34.5548		34.5670	34.5529	34.5800	34.5800	1.245-12
26	2p3p	³ D ₁				34.7028	34.6840	34.7098	34.7097	1.434-12
27	2p3p	³ D ₂	34.8010	34.6993		34.7198	34.7020	34.7274	34.7272	1.906-12
28	2p3p	³ D ₃				34.8474	34.8221	34.8462	34.8459	1.879-12
29	2p3p	³ S ₁		34.9299		34.9529	34.9330	34.9609	34.9604	1.200-12
30	2p3p	³ P ₀				34.9864	34.9730	35.0214	35.0201	1.124-12
31	2p3p	³ P ₁		35.0462		35.0674	35.0477	35.0911	35.0901	1.136-12
32	2p3d	³ F ₂ ^o			35.0998	35.1111	35.0952	35.1303	35.1283	2.943-12
33	2p3p	³ P ₂	35.0750			35.1128	35.0904	35.1364	35.1353	1.113-12
34	2p3d	³ F ₃ ^o		35.1761	35.1814	35.1992	35.1790	35.2181	35.2156	6.466-12
35	2p3d	¹ D ₂ ^o		35.2343		35.2501	35.2279	35.2668	35.2661	7.737-13
36	2p3d	³ F ₄ ^o			35.2810	35.3058	35.2785	35.3132	35.3106	7.852-10
37	2p3p	¹ D ₂		35.3229		35.3762	35.3543	35.4072	35.4031	7.706-13
38	2p3d	³ D ₁ ^o			35.4474	35.4587	35.4393	35.4778	35.4780	2.435-13
39	2p3d	³ D ₂ ^o	35.4940	35.4740	35.4787	35.4923	35.4704	35.5121	35.5122	2.683-13
40	2p3d	³ D ₃ ^o			35.5393	35.5567	35.5303	35.5702	35.5704	2.403-13

Index	Configuration	Level	NIST	MBPT	MCHF	GRASP1	GRASP2	FAC1	FAC2	τ (s)
41	2p3d	$^3P_2^o$			35.6233	35.6450	35.6192	35.6560	35.6558	3.799-13
42	2p3d	$^3P_1^o$		35.6408	35.6450	35.6672	35.6420	35.6794	35.6792	4.088-13
43	2p3d	$^3P_0^o$			35.6596	35.6804	35.6572	35.6949	35.6946	4.375-13
44	2p3p	1S_0		35.7518		35.8426	35.8248	35.8827	35.8703	1.249-12
45	2p3d	$^1F_3^o$	35.9400	35.9322	35.9497	36.0147	35.9882	36.0298	36.0231	1.872-13
46	2p3d	$^1P_1^o$		36.0002	36.0081	36.0624	36.0386	36.0766	36.0743	3.137-13
47	2s4s	3S_1				42.1793	42.1612	42.1662	42.1651	3.058-12
48	2s4s	1S_0				42.3137	42.2962	42.3045	42.3017	3.618-12
49	2s4p	$^3P_0^o$				42.5337	42.5165	42.5269	42.5269	8.031-12
50	2s4p	$^3P_1^o$				42.5387	42.5210	42.5313	42.5313	6.176-12
51	2s4p	$^3P_2^o$				42.5548	42.5361	42.5461	42.5462	8.187-12
52	2s4p	$^1P_1^o$				42.5857	42.5669	42.5792	42.5768	1.024-12
53	2s4d	3D_1				42.7546	42.7356	42.7438	42.7427	7.550-13
54	2s4d	3D_2				42.7571	42.7377	42.7459	42.7448	7.577-13
55	2s4d	3D_3				42.7609	42.7414	42.7495	42.7484	7.617-13
56	2s4d	1D_2				42.8827	42.8635	42.8697	42.8677	8.569-13
57	2s4f	$^3F_2^o$				42.8910	42.8719	42.8786	42.8764	1.795-12
58	2s4f	$^3F_3^o$				42.8922	42.8728	42.8795	42.8773	1.795-12
59	2s4f	$^3F_4^o$				42.8939	42.8743	42.8811	42.8788	1.796-12
60	2s4f	$^1F_3^o$				42.9244	42.9050	42.9129	42.9104	1.826-12
61	2p4s	$^3P_0^o$				44.4581	44.4426	44.4712	44.4713	3.501-12
62	2p4s	$^3P_1^o$				44.4817	44.4655	44.4945	44.4933	3.186-12
63	2p4s	$^3P_2^o$				44.6452	44.6193	44.6463	44.6464	3.156-12
64	2p4p	3D_1				44.7174	44.7015	44.7329	44.7330	1.815-12
65	2p4s	$^1P_1^o$				44.7209	44.6954	44.7249	44.7179	2.399-12
66	2p4p	3D_2				44.7955	44.7773	44.8097	44.8094	2.032-12
67	2p4p	3P_1				44.7960	44.7784	44.8112	44.8100	1.736-12
68	2p4p	3P_0				44.8683	44.8518	44.8916	44.8887	1.913-12
69	2p4d	$^3F_2^o$				44.9356	44.9187	44.9457	44.9439	2.478-12
70	2p4p	3D_3				44.9369	44.9098	44.9499	44.9486	2.103-12
71	2p4p	1P_1				44.9387	44.9135	44.9395	44.9396	1.680-12
72	2p4d	$^3F_3^o$				44.9982	44.9794	45.0127	45.0114	1.708-12
73	2p4p	3P_2				45.0016	44.9760	45.0104	45.0070	1.874-12
74	2p4p	3S_1				45.0019	44.9762	45.0105	45.0088	1.756-12
75	2p4d	$^3D_2^o$				45.0139	44.9958	45.0265	45.0256	9.595-13
76	2p4d	$^3D_1^o$				45.0634	45.0454	45.0748	45.0741	6.067-13
77	2p4f	3G_3				45.0846	45.0671	45.0942	45.0910	1.816-12
78	2p4p	1D_2				45.0857	45.0636	45.1223	45.1193	1.672-12
79	2p4f	3F_3				45.0937	45.0761	45.1034	45.1034	1.817-12
80	2p4f	3G_4				45.0975	45.0799	45.1074	45.1040	1.867-12

Index	Configuration	Level	NIST	MBPT	MCHF	GRASP1	GRASP2	FAC1	FAC2	τ (s)
81	2p4f	3F_2				45.1092	45.0878	45.0974	45.0961	1.671-12
82	2p4d	$^3F_4^o$				45.1288	45.1013	45.1312	45.1295	3.697-12
83	2p4d	$^1D_2^o$				45.1504	45.1242	45.1536	45.1528	9.341-13
84	2p4d	$^3D_3^o$				45.1926	45.1656	45.1942	45.1940	6.453-13
85	2p4d	$^3P_2^o$				45.2271	45.2000	45.2286	45.2272	7.548-13
86	2p4d	$^3P_1^o$				45.2371	45.2103	45.2391	45.2370	8.236-13
87	2p4d	$^3P_0^o$				45.2437	45.2178	45.2467	45.2441	9.210-13
88	2p4f	1F_3				45.2561	45.2288	45.2545	45.2524	1.814-12
89	2p4f	3F_4				45.2639	45.2366	45.2623	45.2599	1.838-12
90	2p4p	1S_0				45.2835	45.2594	45.2920	45.2774	2.414-12
91	2p4f	3G_5				45.2926	45.2648	45.2989	45.2842	1.830-12
92	2p4f	3D_3				45.2929	45.2661	45.3094	45.2921	1.807-12
93	2p4f	3D_2				45.2993	45.2725	45.2903	45.2988	1.807-12
94	2p4f	1G_4				45.3119	45.2842	45.3107	45.3042	1.955-12
95	2p4f	3D_1				45.3289	45.3020	45.3280	45.3281	1.801-12
96	2p4f	1D_2				45.3444	45.3174	45.3441	45.3438	1.807-12
97	2p4d	$^1F_3^o$				45.3605	45.3338	45.3604	45.3527	4.311-13
98	2p4d	$^1P_1^o$				45.3767	45.3510	45.3775	45.3721	6.594-13

NIST: <http://www.nist.gov/pml/data/asd.cfm>

MBPT: Gu [29] for the lowest 10 levels and Safronova *et al* [30] for the remaining levels

MCHF: Calculations of C Froese Fischer (2009) available at <http://nlte.nist.gov/MCHF/view.html>

GRASP1: Coulomb energies

GRASP2: QED corrected energies

FAC1: Energies from the FAC for 98 level calculations

FAC2: Energies from the FAC for 166 level calculations

Table 2: Energy levels (in Ryd) of K XVI and their lifetimes (τ , s). $a \pm b \equiv a \times 10^{\pm b}$.

Index	Configuration	Level	NIST	MBPT	GRASP1	GRASP2	FAC1	FAC2	τ (s)
1	2s ²	¹ S ₀	0.0000	0.0000	0.0000	0.0000	0.0000	0.0000
2	2s2p	³ P ₀ ^o	2.2191	2.2198	2.2183	2.2241	2.2325	2.2319
3	2s2p	³ P ₁ ^o	2.3011	2.3023	2.3079	2.3064	2.3143	2.3137	2.421-07
4	2s2p	³ P ₂ ^o	2.4977	2.4994	2.5141	2.5023	2.5092	2.5087	7.442-03
5	2s2p	¹ P ₁ ^o	4.4178	4.4157	4.5028	4.4974	4.4959	4.4911	9.267-11
6	2p ²	³ P ₀	5.8933	5.8947	5.9272	5.9301	5.9481	5.9473	1.285-10
7	2p ²	³ P ₁	6.0162	6.0174	6.0539	6.0508	6.0681	6.0674	1.217-10
8	2p ²	³ P ₂	6.1647	6.1663	6.2176	6.2005	6.2171	6.2162	1.195-10
9	2p ²	¹ D ₂	6.7675	6.7641	6.8594	6.8442	6.8596	6.8557	4.047-10
10	2p ²	¹ S ₀	8.2266	8.2241	8.3640	8.3631	8.3716	8.3689	5.888-11
11	2s3s	³ S ₁		40.5331	40.5355	40.5139	40.5127	40.5125	9.796-13
12	2s3s	¹ S ₀		40.9544	40.9582	40.9378	40.9509	40.9507	2.792-12
13	2s3p	¹ P ₁ ^o	41.5890	41.5561	41.5694	41.5481	41.5593	41.5587	5.487-13
14	2s3p	³ P ₀ ^o			41.5822	41.5635	41.5751	41.5753	6.808-11
15	2s3p	³ P ₁ ^o		41.6281	41.6410	41.6174	41.6282	41.6279	7.904-13
16	2s3p	³ P ₂ ^o			41.6656	41.6420	41.6526	41.6528	5.444-11
17	2s3d	³ D ₁			42.2243	42.1983	42.2126	42.2104	1.766-13
18	2s3d	³ D ₂	42.2460	42.2187	42.2359	42.2084	42.2225	42.2203	1.783-13
19	2s3d	³ D ₃	42.2550		42.2533	42.2249	42.2389	42.2366	1.805-13
20	2s3d	¹ D ₂	42.6380	42.6222	42.6760	42.6494	42.6626	42.6586	2.584-13
21	2p3s	³ P ₀ ^o			43.3296	43.3118	43.3380	43.3381	1.301-12
22	2p3s	³ P ₁ ^o		43.3811	43.3987	43.3780	43.4042	43.4041	1.239-12
23	2p3s	³ P ₂ ^o			43.6320	43.5989	43.6234	43.6235	1.182-12
24	2p3s	¹ P ₁ ^o		43.9353	43.9969	43.9674	43.9982	43.9945	9.444-13
25	2p3p	³ D ₁			44.0149	43.9961	44.0234	44.0234	8.080-13
26	2p3p	¹ P ₁		43.9971	44.2220	44.1957	44.2220	44.2220	7.785-13
27	2p3p	³ D ₂		44.2017	44.2280	44.2029	44.2288	44.2285	1.085-12
28	2p3p	³ D ₃	44.4200		44.4434	44.4068	44.4306	44.4304	1.074-12
29	2p3p	³ P ₀			44.5099	44.4913	44.5400	44.5386	6.573-13
30	2p3p	³ S ₁		44.4942	44.5255	44.4961	44.5254	44.5250	7.008-13
31	2p3d	³ F ₂ ^o			44.6584	44.6356	44.6707	44.6688	1.714-12
32	2p3p	³ P ₁		44.6337	44.6651	44.6355	44.6764	44.6754	6.717-13
33	2p3p	³ P ₂			44.7225	44.6903	44.7360	44.7348	6.444-13
34	2p3d	³ F ₃ ^o		44.7634	44.7947	44.7663	44.8055	44.8031	2.114-12
35	2p3d	¹ D ₂ ^o		44.8466	44.8706	44.8404	44.8797	44.8791	4.040-13
36	2p3d	³ F ₄ ^o			44.9790	44.9396	44.9739	44.9713	4.452-10
37	2p3p	¹ D ₂		44.9660	45.0283	44.9959	45.0481	45.0442	4.606-13
38	2p3d	³ D ₁ ^o			45.0766	45.0495	45.0877	45.0878	1.478-13
39	2p3d	³ D ₂ ^o	45.1810	45.1199	45.1492	45.1164	45.1570	45.1570	1.758-13
40	2p3d	³ D ₃ ^o	45.2500		45.2543	45.2159	45.2554	45.2555	1.464-13

Index	Configuration	Level	NIST	MBPT	GRASP1	GRASP2	FAC1	FAC2	τ (s)
41	2p3d	$^3P_2^o$			45.3568	45.3189	45.3556	45.3555	2.148-13
42	2p3d	$^3P_1^o$		45.3443	45.3819	45.3452	45.3826	45.3825	2.354-13
43	2p3d	$^3P_0^o$			45.3986	45.3652	45.4026	45.4024	2.595-13
44	2p3p	1S_0		45.4588	45.5575	45.5310	45.5886	45.5764	7.079-13
45	2p3d	$^1F_3^o$	45.7120	45.6848	45.7785	45.7397	45.7808	45.7743	1.112-13
46	2p3d	$^1P_1^o$		45.7565	45.8293	45.7945	45.8321	45.8299	1.856-13
47	2s4s	3S_1			54.2989	54.2733	54.2781	54.2770	1.873-12
48	2s4s	1S_0			54.4509	54.4262	54.4343	54.4316	2.271-12
49	2s4p	$^3P_0^o$			54.7057	54.6814	54.6916	54.6917	4.641-12
50	2s4p	$^3P_1^o$			54.7129	54.6879	54.6981	54.6980	3.098-12
51	2s4p	$^3P_2^o$			54.7407	54.7143	54.7239	54.7241	4.752-12
52	2s4p	$^1P_1^o$			54.7740	54.7474	54.7592	54.7569	6.286-13
53	2s4d	3D_1			54.9710	54.9440	54.9520	54.9509	4.507-13
54	2s4d	3D_2			54.9751	54.9476	54.9555	54.9544	4.528-13
55	2s4d	3D_3			54.9816	54.9538	54.9617	54.9606	4.561-13
56	2s4d	1D_2			55.1184	55.0911	55.0971	55.0950	5.110-13
57	2s4f	$^3F_2^o$			55.1308	55.1036	55.1103	55.1079	1.058-12
58	2s4f	$^3F_3^o$			55.1328	55.1052	55.1118	55.1094	1.058-12
59	2s4f	$^3F_4^o$			55.1358	55.1079	55.1145	55.1121	1.059-12
60	2s4f	$^1F_3^o$			55.1696	55.1420	55.1497	55.1471	1.078-12
61	2p4s	$^3P_0^o$			56.8894	56.8672	56.8958	56.8959	2.197-12
62	2p4s	$^3P_1^o$			56.9187	56.8958	56.9249	56.9236	1.951-12
63	2p4p	3D_1			57.1880	57.1655	57.1970	57.1971	1.099-12
64	2p4s	$^3P_2^o$			57.1951	57.1579	57.1845	57.1847	1.883-12
65	2p4s	$^1P_1^o$			57.2776	57.2408	57.2697	57.2637	1.512-12
66	2p4p	3P_1			57.2945	57.2703	57.3039	57.3025	1.048-12
67	2p4p	3D_2			57.2962	57.2709	57.3040	57.3035	1.177-12
68	2p4p	3P_0			57.3702	57.3474	57.3877	57.3841	1.126-12
69	2p4d	$^3F_2^o$			57.4495	57.4253	57.4565	57.4552	1.452-12
70	2p4p	1P_1			57.5335	57.4964	57.5276	57.5267	9.950-13
71	2p4d	$^3F_3^o$			57.5359	57.5096	57.5406	57.5389	8.382-13
72	2p4p	3D_3			57.5417	57.5028	57.5320	57.5322	1.234-12
73	2p4d	$^3D_2^o$			57.5490	57.5237	57.5543	57.5535	5.351-13
74	2p4p	3P_2			57.6018	57.5651	57.6009	57.5996	1.096-12
75	2p4d	$^3D_1^o$			57.6025	57.5771	57.6065	57.6057	3.680-13
76	2p4p	3S_1			57.6076	57.5706	57.6040	57.6006	1.040-12
77	2p4f	3G_3			57.6251	57.6001	57.6273	57.6241	1.069-12
78	2p4f	3F_3			57.6390	57.6139	57.6413	57.6414	1.069-12
79	2p4f	3F_2			57.6402	57.6143	57.6424	57.6425	1.080-12
80	2p4f	3G_4			57.6422	57.6171	57.6447	57.6414	1.098-12

Index	Configuration	Level	NIST	MBPT	GRASP1	GRASP2	FAC1	FAC2	τ (s)
81	2p4p	1D_2			57.7208	57.6837	57.7233	57.7192	9.315-13
82	2p4d	$^3F_4^o$			57.7661	57.7264	57.7558	57.7542	2.166-12
83	2p4d	$^1D_2^o$			57.7837	57.7452	57.7742	57.7735	6.175-13
84	2p4d	$^3D_3^o$			57.8344	57.7951	57.8234	57.8231	4.084-13
85	2p4d	$^3P_2^o$			57.8761	57.8368	57.8650	57.8639	4.466-13
86	2p4d	$^3P_1^o$			57.8864	57.8476	57.8760	57.8743	4.830-13
87	2p4d	$^3P_0^o$			57.8941	57.8567	57.8852	57.8830	5.481-13
88	2p4f	1F_3			57.9122	57.8727	57.8981	57.8964	1.067-12
89	2p4p	1S_0			57.9207	57.8857	57.9342	57.9065	1.358-12
90	2p4f	3F_4			57.9223	57.8827	57.9081	57.9062	1.079-12
91	2p4f	3D_3			57.9533	57.9142	57.9398	57.9399	1.064-12
92	2p4f	3G_5			57.9567	57.9165	57.9417	57.9362	1.076-12
93	2p4f	3D_2			57.9588	57.9198	57.9458	57.9458	1.065-12
94	2p4f	1G_4			57.9778	57.9377	57.9639	57.9581	1.138-12
95	2p4f	3D_1			57.9965	57.9577	57.9834	57.9835	1.060-12
96	2p4f	1D_2			58.0150	57.9760	58.0023	58.0020	1.065-12
97	2p4d	$^1F_3^o$			58.0209	57.9818	58.0081	58.0013	2.652-13
98	2p4d	$^1P_1^o$			58.0413	58.0037	58.0299	58.0251	3.988-13

NIST: <http://www.nist.gov/pml/data/asd.cfm>

MBPT: Gu [29] for the lowest 10 levels and Safronova *et al* [30] for the remaining levels

GRASP1: Coulomb energies

GRASP2: QED corrected energies

FAC1: Energies from the FAC for 98 level calculations

FAC2: Energies from the FAC for 166 level calculations

Table 3: Energy levels (in Ryd) of Ge XXIX and their lifetimes (τ , s). $a \pm b \equiv a \times 10^{\pm b}$.

Index	Configuration	Level	NIST	MBPT	GRASP1	GRASP2	FAC1	FAC2	τ (s)
1	2s ²	¹ S ₀	0.0000	0.0000	0.0000	0.0000	0.0000	0.0000
2	2s2p	³ P ₀ ^o		4.0218	4.0076	4.0261	4.0356	4.0349
3	2s2p	³ P ₁ ^o	4.5709	4.5745	4.5941	4.5830	4.5913	4.5903	4.912-09
4	2s2p	³ P ₂ ^o	6.8006	6.8054	6.8820	6.8037	6.8104	6.8099	5.524-06
5	2s2p	¹ P ₁ ^o	9.8089	9.8159	9.9459	9.8887	9.8874	9.8828	2.720-11
6	2p ²	³ P ₀		11.3155	11.3508	11.3709	11.3898	11.3883	5.842-11
7	2p ²	³ P ₁		13.2583	13.3369	13.2925	13.3102	13.3092	3.607-11
8	2p ²	³ P ₂		13.8769	14.0243	13.9304	13.9470	13.9446	4.777-11
9	2p ²	¹ D ₂		16.5374	16.7319	16.5921	16.6061	16.6036	3.584-11
10	2p ²	¹ S ₀		18.8739	19.0658	18.9956	19.0050	19.0025	1.650-11
11	2s3s	³ S ₁			127.6944	127.5775	127.5759	127.5758	1.109-13
12	2s3s	¹ S ₀			128.4947	128.3840	128.3968	128.3965	2.659-13
13	2s3p	³ P ₀ ^o			129.6281	129.5241	129.5353	129.5354	1.260-11
14	2s3p	³ P ₁ ^o			129.6476	129.5327	129.5436	129.5432	8.841-14
15	2s3p	¹ P ₁ ^o			130.4135	130.2782	130.2887	130.2880	4.847-14
16	2s3p	³ P ₂ ^o			130.4565	130.3238	130.3324	130.3326	5.071-12
17	2s3d	³ D ₁			131.4705	131.3240	131.3359	131.3336	1.707-14
18	2s3d	³ D ₂			131.5755	131.4205	131.4318	131.4294	1.786-14
19	2s3d	³ D ₃			131.7543	131.5955	131.6060	131.6036	1.859-14
20	2s3d	¹ D ₂			132.4454	132.2961	132.3068	132.3025	2.393-14
21	2p3s	³ P ₀ ^o			132.7847	132.6789	132.7063	132.7065	1.657-13
22	2p3s	³ P ₁ ^o			133.0541	132.9407	132.9691	132.9681	1.259-13
23	2p3p	³ D ₁			134.0904	133.9808	134.0095	134.0094	9.384-14
24	2p3p	³ P ₀			135.2060	135.1068	135.1604	135.1568	5.901-14
25	2p3p	¹ P ₁			135.3264	135.2010	135.2351	135.2347	6.822-14
26	2p3p	³ D ₂			135.3576	135.2211	135.2537	135.2528	7.587-14
27	2p3s	³ P ₂ ^o			135.6714	135.4818	135.5069	135.5070	9.257-14
28	2p3d	³ F ₂ ^o			135.9503	135.8111	135.8456	135.8439	1.429-13
29	2p3s	¹ P ₁ ^o			136.1703	135.9858	136.0135	136.0108	1.083-13
30	2p3d	³ F ₃ ^o			136.6778	136.5256	136.5655	136.5632	3.471-14
31	2p3d	³ D ₂ ^o			136.7639	136.6154	136.6544	136.6544	2.380-14
32	2p3d	³ D ₁ ^o			136.8493	136.7010	136.7379	136.7377	1.543-14
33	2p3p	³ P ₁			137.4442	137.2616	137.2978	137.2971	6.117-14
34	2p3p	³ P ₂			137.6575	137.4645	137.5062	137.5043	5.651-14
35	2p3p	³ D ₃			137.8754	137.6606	137.6824	137.6823	8.289-14
36	2p3p	³ S ₁			137.9585	137.7517	137.7753	137.7751	6.455-14
37	2p3p	¹ D ₂			138.7900	138.5838	138.6296	138.6271	5.369-14
38	2p3d	¹ D ₂ ^o			139.0858	138.8646	138.8996	138.8991	2.864-14
39	2p3d	³ F ₄ ^o			139.0920	138.8618	138.8920	138.8895	1.991-11
40	2p3d	³ D ₃ ^o			139.3807	139.1487	139.1842	139.1831	1.895-14

Index	Configuration	Level	NIST	MBPT	GRASP1	GRASP2	FAC1	FAC2	τ (s)
41	2p3d	$^3P_1^o$		139.6025	139.3823	139.4176	139.4176	1.996-14	
42	2p3d	$^3P_0^o$		139.6248	139.4278	139.4622	139.4620	2.437-14	
43	2p3p	1S_0		139.6518	139.4719	139.5251	139.5150	6.259-14	
44	2p3d	$^3P_2^o$		139.6640	139.4373	139.4706	139.4706	1.986-14	
45	2p3d	$^1F_3^o$		140.3344	140.0968	140.1331	140.1278	1.135-14	
46	2p3d	$^1P_1^o$		140.4891	140.2742	140.3078	140.3060	1.790-14	
47	2s4s	3S_1		171.5349	171.3948	171.3980	171.3969	2.004-13	
48	2s4s	1S_0		171.8124	171.6756	171.6823	171.6796	2.454-13	
49	2s4p	$^3P_0^o$		172.2952	172.1604	172.1693	172.1693	4.057-13	
50	2s4p	$^3P_1^o$		172.3205	172.1817	172.1910	172.1903	1.607-13	
51	2s4p	$^3P_2^o$		172.6433	172.4966	172.5040	172.5042	4.333-13	
52	2s4p	$^1P_1^o$		172.6955	172.5474	172.5566	172.5546	7.385-14	
53	2s4d	3D_1		173.0713	172.9192	172.9248	172.9236	4.396-14	
54	2s4d	3D_2		173.1060	172.9508	172.9563	172.9551	4.470-14	
55	2s4d	3D_3		173.1793	173.0227	173.0282	173.0270	4.573-14	
56	2s4d	1D_2		173.3942	173.2410	173.2448	173.2425	4.935-14	
57	2s4f	$^3F_2^o$		173.4504	173.2973	173.3016	173.2990	9.927-14	
58	2s4f	$^3F_3^o$		173.4647	173.3084	173.3128	173.3100	9.945-14	
59	2s4f	$^3F_4^o$		173.5014	173.3446	173.3487	173.3459	9.976-14	
60	2s4f	$^1F_3^o$		173.5498	173.3952	173.4003	173.3974	1.010-13	
61	2p4s	$^3P_0^o$		176.2662	176.1341	176.1631	176.1633	2.553-13	
62	2p4s	$^3P_1^o$		176.3284	176.1939	176.2237	176.2220	2.105-13	
63	2p4p	3D_1		176.8300	176.6953	176.7273	176.7274	1.074-13	
64	2p4p	3P_0		177.2203	177.0916	177.1357	177.1284	1.033-13	
65	2p4p	3S_1		177.3232	177.1834	177.2181	177.2166	1.048-13	
66	2p4p	3D_2		177.3510	177.2064	177.2416	177.2403	1.060-13	
67	2p4d	$^3F_2^o$		177.6001	177.4533	177.4840	177.4830	1.322-13	
68	2p4d	$^3D_2^o$		177.8708	177.7217	177.7517	177.7512	4.637-14	
69	2p4d	$^3F_3^o$		177.9047	177.7533	177.7831	177.7811	5.176-14	
70	2p4d	$^3D_1^o$		177.9089	177.7607	177.7895	177.7882	3.731-14	
71	2p4f	3G_3		178.0126	177.8619	177.8886	177.8860	1.001-13	
72	2p4f	3D_2		178.0515	177.9017	177.9289	177.9290	1.000-13	
73	2p4f	3D_3		178.0844	177.9344	177.9612	177.9614	1.001-13	
74	2p4f	3G_4		178.0891	177.9380	177.9650	177.9623	1.020-13	
75	2p4s	$^3P_2^o$		179.2174	179.0020	179.0261	179.0262	2.736-13	
76	2p4s	$^1P_1^o$		179.3263	179.1121	179.1379	179.1337	1.765-13	
77	2p4p	3P_1		179.9074	179.6942	179.7251	179.7240	9.880-14	
78	2p4p	1D_2		179.9606	179.7436	179.7764	179.7746	1.001-13	
79	2p4p	3D_3		180.1395	179.9136	179.9397	179.9399	1.132-13	
80	2p4p	1P_1		180.1659	179.9429	179.9701	179.9677	9.841-14	

Index	Configuration	Level	NIST	MBPT	GRASP1	GRASP2	FAC1	FAC2	τ (s)
81	2p4p	3P_2			180.4185	180.1963	180.2311	180.2285	9.909-14
82	2p4d	$^1D_2^o$			180.6077	180.3794	180.4051	180.4046	6.246-14
83	2p4d	$^3F_4^o$			180.6447	180.4125	180.4386	180.4371	2.002-13
84	2p4d	$^3D_3^o$			180.7003	180.4682	180.4935	180.4924	4.998-14
85	2p4p	1S_0			180.7277	180.5151	180.5569	180.5381	1.145-13
86	2p4d	$^3P_1^o$			180.7771	180.5492	180.5744	180.5732	4.456-14
87	2p4d	$^3P_0^o$			180.7878	180.5683	180.5936	180.5917	5.243-14
88	2p4d	$^3P_2^o$			180.8098	180.5796	180.6045	180.6036	4.627-14
89	2p4f	3F_3			180.9192	180.6877	180.7099	180.7088	9.974-14
90	2p4f	3F_4			180.9668	180.7341	180.7562	180.7545	1.004-13
91	2p4f	3F_2			180.9906	180.7605	180.7832	180.7833	9.969-14
92	2p4f	1F_3			181.0208	180.7901	180.8123	180.8124	9.990-14
93	2p4d	$^1F_3^o$			181.0308	180.7972	180.8205	180.8160	2.891-14
94	2p4f	3G_5			181.0437	180.8091	180.8310	180.8263	1.008-13
95	2p4f	1G_4			181.0536	180.8190	180.8420	180.8374	1.033-13
96	2p4f	3D_1			181.0726	180.8457	180.8682	180.8684	9.919-14
97	2p4d	$^1P_1^o$			181.0995	180.8745	180.8978	180.8941	4.107-14
98	2p4f	1D_2			181.1437	180.9151	180.9379	180.9379	1.002-13

NIST: <http://www.nist.gov/pml/data/asd.cfm>

MBPT: Gu [29] for the lowest 10 levels and Safronova *et al* [30] for the remaining levels

GRASP1: Coulomb energies

GRASP2: QED corrected energies

FAC1: Energies from the FAC for 98 level calculations

FAC2: Energies from the FAC for 166 level calculations

Table 7: Comparisons of oscillator strengths (f - values) for E1 transitions from the lowest 5 levels of Cl XIV and K XVI. $a \pm b \equiv a \times 10^{\pm b}$.

Transition		Cl XIV			K XVI		
I	J	GRASP	MCHF	R	GRASP	MCHF	R
1	3	1.534–4	1.688–4	0.81	2.901–4	3.148–4	0.85
1	5	2.216–1	2.173–1	0.98	1.992–1	1.958–1	0.99
1	13	4.503–1	4.867–1	0.98	3.753–1	4.093–1	0.98
1	15	1.643–1	1.318–1	0.98	2.581–1	2.272–1	0.98
1	22	1.584–3	1.609–3	1.10	3.086–3	3.095–3	1.00
1	24	2.692–2	2.326–2	1.10	2.769–2	2.431–2	1.10
1	38	8.779–4	1.041–3	1.00	1.613–3	1.857–3	1.00
1	42	1.240–4	1.458–4	1.00	1.592–4	1.826–4	1.00
1	46	2.696–2	2.891–2	1.10	2.550–2	2.714–2	1.10
2	7	8.602–2	8.493–2	0.93	7.802–2	7.714–2	0.93
2	11	2.986–2	2.978–2	0.96	2.873–2	2.869–2	0.97
2	17	7.309–1	7.300–1	0.98	7.372–1	7.362–1	0.99
3	6	2.757–2	2.721–2	0.92	2.458–2	2.430–2	0.92
3	7	2.110–2	2.082–2	0.92	1.897–2	1.875–2	0.93
3	8	3.645–2	3.597–2	0.93	3.325–2	3.283–2	0.94
3	9	1.523–4	1.996–4	0.68	3.181–4	3.980–4	0.72
3	10	1.676–5	2.056–5	1.70	2.827–5	3.368–5	1.80
3	11	3.004–2	2.999–2	0.96	2.891–2	2.889–2	0.97
3	12	6.206–6	4.291–6	0.62	1.277–5	9.890–6	0.68
3	17	1.823–1	1.822–1	0.98	1.835–1	1.833–1	0.99
3	18	5.459–1	5.455–1	0.98	5.493–1	5.488–1	0.99
3	20	2.679–4	2.538–4	1.00	5.476–4	5.245–4	1.00
4	7	2.028–2	2.000–2	0.92	1.794–2	1.772–2	0.92
4	8	6.160–2	6.056–2	0.92	5.382–2	5.279–2	0.93
4	9	1.576–3	1.822–3	0.94	3.008–3	3.397–3	0.95
4	11	3.040–2	3.051–2	0.96	2.936–2	2.948–2	0.97
4	17	7.301–3	7.303–3	0.98	7.350–3	7.351–3	0.99
4	18	1.091–1	1.092–1	0.98	1.098–1	1.098–1	0.99
4	19	6.090–1	6.092–1	0.98	6.119–1	6.120–1	0.99
4	20	2.022–5	2.562–5	0.98	4.513–5	5.547–5	0.98
5	6	4.977–5	5.637–5	0.02	8.619–5	9.569–5	0.03
5	7	1.464–5	1.647–5	0.76	2.785–5	3.080–5	0.79
5	8	9.025–4	1.106–3	1.50	1.816–3	2.152–3	1.40
5	9	8.253–2	8.157–2	1.30	7.475–2	7.378–2	1.30
5	10	5.284–2	5.090–2	0.61	4.710–2	4.558–2	0.63
5	11	5.361–5	6.083–5	0.98	1.047–4	1.159–4	0.99
5	12	1.175–2	1.015–2	0.84	1.118–2	9.838–3	0.86
5	17	2.754–4	3.086–4	1.00	5.749–4	6.329–4	1.00
5	18	3.304–4	3.471–4	0.98	6.738–4	6.991–4	0.98
5	20	5.483–1	5.359–1	1.00	5.504–1	5.393–1	1.00

GRASP: Present results from the GRASP code

MCHF: Earlier results of C Froese Fischer (2009) from the MCHF code available at the website <http://nle.nist.gov/MCHF/view.html>

R: ratio of the velocity and length form of the f- values from the GRASP code

Table 8: Comparisons of radiative rates (A- values, s^{-1}) for M1 and M2 transitions of Cl XIV and K XVI.

$a \pm b \equiv a \times 10^{\pm b}$.

Transition	Type	Cl XIV		K XVI	
		GRASP	MBPT	GRASP	MBPT
I	J				
1	4	M2	5.96–1	5.85–1	1.05–0
1	7	M1	1.55+2	1.49+2	4.79+2
2	3	M1	3.13–0	3.16–0	1.32+1
2	5	M1	3.19+2	2.60+2	1.04+3
3	4	M1	2.83+1	2.89+1	1.33+2
3	5	M1	2.28+2	1.85+2	7.14+2
4	5	M1	3.10+2	2.50+2	8.92+2
6	7	M1	7.40–0	7.79–0	4.11+1
7	8	M1	1.51+1	1.50+1	5.72+1
7	9	M1	1.05+2	6.99+1	3.95+2
7	10	M1	3.24+3	2.55+3	9.97+3
8	9	M1	1.94+2	1.25+2	8.15+3
					4.27+2

GRASP: Present results from the GRASP code

MBPT: Results of Safronova *et al* [17] from the *many-body perturbation theory* for M1 transitions and of Safronova [35] for the M2

Table 9: Comparison of lifetimes (τ) among the lowest 10 levels of Cl XIV.

Level	GRASP	MBPT	Experimental
3	605.2 ns
4	34.64 ms
5	110.0 ps	116 ^a	150±30 [19], 140±10 [20], 117±10 [23]
6	150.0 ps	227	170±9 [23]
7	144.9 ps	224	170±10 [19], 160±10 [20], 165±15 [23]
8	141.5 ps	220	160±10 [19], 169±5 [20], 160±10 [23]
9	567.7 ps	...	600±60 [19], 630±20 [20] 625±25 [23], 540±10 [18], 600 [21]
10	70.51 ps	...	84±5 [19], 77±9 [23]

GRASP: present results with the GRASP code

MBPT: Saforonova *et al* [16] with the MBPT code

a: Andersson *et al* [36]

Table 10: Collision strengths for the resonance transitions of Cl XIV. ($a \pm b \equiv a \times 10^{\pm b}$).

Transition		Energy (Ryd)						
<i>i</i>	<i>j</i>	100	200	300	400	500	600	700
1	2	7.813–04	3.038–04	1.605–04	9.920–05	6.739–05	4.870–05	3.698–05
1	3	4.405–03	2.874–03	2.416–03	2.235–03	2.018–03	1.917–03	1.851–03
1	4	3.859–03	1.497–03	7.903–04	4.880–04	3.314–04	2.394–04	1.817–04
1	5	1.202–00	1.282–00	1.281–00	1.332–00	1.221–00	1.188–00	1.176–00
1	6	4.014–05	2.490–05	2.097–05	1.940–05	1.862–05	1.819–05	1.790–05
1	7	5.330–05	1.470–05	6.014–06	3.037–06	1.750–06	1.100–06	7.350–07
1	8	2.201–04	1.715–04	1.635–04	1.619–04	1.619–04	1.623–04	1.632–04
1	9	5.152–03	5.519–03	5.699–03	5.800–03	5.867–03	5.913–03	5.964–03
1	10	1.846–03	1.615–03	1.503–03	1.438–03	1.395–03	1.368–03	1.347–03
1	11	6.144–04	2.048–04	1.023–04	6.143–05	4.100–05	2.941–05	2.213–05
1	12	3.855–02	4.152–02	4.266–02	4.334–02	4.383–02	4.423–02	4.458–02
1	13	3.957–02	6.696–02	8.557–02	1.001–01	1.106–01	1.200–01	1.285–01
1	14	1.627–04	4.635–05	2.124–05	1.207–05	7.750–06	5.386–06	3.945–06
1	15	1.628–02	2.724–02	3.479–02	4.069–02	4.500–02	4.882–02	5.226–02
1	16	8.057–04	2.295–04	1.052–04	5.974–05	3.835–05	2.664–05	1.951–05
1	17	8.754–04	2.537–04	1.173–04	6.698–05	4.313–05	3.003–05	2.208–05
1	18	1.479–03	4.478–04	2.226–04	1.400–04	1.010–04	7.956–05	6.670–05
1	19	2.043–03	5.920–04	2.737–04	1.563–04	1.006–04	7.006–05	5.151–05
1	20	7.541–02	9.605–02	1.045–01	1.091–01	1.119–01	1.136–01	1.151–01
1	21	2.968–06	9.053–07	4.205–07	2.392–07	1.530–07	1.059–07	7.768–08
1	22	1.526–04	2.482–04	3.169–04	3.709–04	4.112–04	4.463–04	4.783–04
1	23	1.408–05	4.310–06	2.004–06	1.141–06	7.312–07	5.067–07	3.721–07
1	24	2.179–03	3.688–03	4.738–03	5.557–03	6.168–03	6.698–03	7.179–03
1	25	3.686–05	1.836–05	1.207–05	8.897–06	6.986–06	5.714–06	4.811–06
1	26	3.347–05	1.492–05	9.216–06	6.542–06	5.011–06	4.028–06	3.348–06
1	27	6.565–05	3.166–05	2.353–05	2.055–05	1.918–05	1.845–05	1.806–05
1	28	7.030–05	2.288–05	1.091–05	6.287–06	4.058–06	2.825–06	2.076–06
1	29	2.062–05	7.182–06	3.759–06	2.380–06	1.676–06	1.262–06	9.955–07
1	30	6.888–06	4.569–06	4.147–06	4.024–06	3.980–06	3.968–06	3.968–06
1	31	1.049–05	2.748–06	1.157–06	6.156–07	3.761–07	2.513–07	1.788–07
1	32	3.523–05	1.427–05	9.753–06	7.777–06	6.607–06	5.803–06	5.206–06
1	33	4.366–05	4.128–05	4.232–05	4.319–05	4.379–05	4.418–05	4.453–05
1	34	4.609–05	1.698–05	1.167–05	9.941–06	9.216–06	8.870–06	8.699–06
1	35	4.435–05	2.994–05	2.541–05	2.239–05	2.008–05	1.823–05	1.671–05
1	36	4.996–05	1.273–05	5.610–06	3.140–06	2.006–06	1.393–06	1.025–06
1	37	5.882–04	7.366–04	7.904–04	8.162–04	8.305–04	8.390–04	8.460–04
1	38	1.638–04	2.200–04	2.597–04	2.905–04	3.139–04	3.340–04	3.521–04
1	39	2.112–05	6.313–06	3.436–06	2.375–06	1.843–06	1.524–06	1.311–06
1	40	1.558–05	7.302–06	6.302–06	6.133–06	6.134–06	6.180–06	6.240–06
1	41	5.069–05	1.419–05	6.591–06	3.837–06	2.540–06	1.825–06	1.387–06
1	42	5.335–05	3.667–05	3.661–05	3.862–05	4.068–05	4.267–05	4.461–05
1	43	1.213–05	3.371–06	1.532–06	8.671–07	5.560–07	3.862–07	2.836–07
1	44	1.962–04	1.929–04	1.927–04	1.932–04	1.937–04	1.944–04	1.951–04
1	45	4.648–04	5.228–04	5.495–04	5.667–04	5.794–04	5.894–04	5.981–04
1	46	4.157–03	5.819–03	6.912–03	7.748–03	8.383–03	8.918–03	9.401–03

Table 10: Collision strengths for the resonance transitions of Cl XIV. ($a \pm b \equiv a \times 10^{\pm b}$).

Transition		Energy (Ryd)						
<i>i</i>	<i>j</i>	100	200	300	400	500	600	700
1	47	2.386–04	7.346–05	3.558–05	2.099–05	1.389–05	9.847–06	7.396–06
1	48	7.479–03	8.263–03	8.565–03	8.737–03	8.860–03	8.957–03	9.040–03
1	49	7.504–05	1.935–05	8.501–06	4.711–06	2.983–06	2.044–06	1.486–06
1	50	7.339–04	9.332–04	1.144–03	1.318–03	1.461–03	1.577–03	1.685–03
1	51	3.720–04	9.588–05	4.210–05	2.332–05	1.476–05	1.011–05	7.352–06
1	52	1.080–02	1.838–02	2.351–02	2.742–02	3.057–02	3.308–02	3.543–02
1	53	3.416–04	9.522–05	4.344–05	2.463–05	1.580–05	1.096–05	8.047–06
1	54	5.743–04	1.658–04	8.037–05	4.943–05	3.497–05	2.710–05	2.237–05
1	55	7.955–04	2.216–04	1.011–04	5.730–05	3.675–05	2.550–05	1.872–05
1	56	1.255–02	1.632–02	1.785–02	1.868–02	1.920–02	1.956–02	1.984–02
1	57	1.652–04	3.516–05	1.432–05	7.660–06	4.751–06	3.232–06	2.340–06
1	58	2.373–04	5.705–05	2.835–05	1.924–05	1.528–05	1.324–05	1.206–05
1	59	2.966–04	6.305–05	2.567–05	1.373–05	8.515–06	5.792–06	4.194–06
1	60	4.502–03	5.444–03	5.702–03	5.819–03	5.891–03	5.939–03	5.986–03
1	61	1.349–06	3.873–07	1.766–07	9.980–08	6.376–08	4.412–08	3.241–08
1	62	1.906–05	2.328–05	2.747–05	3.086–05	3.362–05	3.584–05	3.786–05
1	63	6.485–06	1.893–06	8.699–07	4.940–07	3.169–07	2.201–07	1.621–07
1	64	9.316–06	3.467–06	2.005–06	1.387–06	1.052–06	8.440–07	7.026–07
1	65	6.471–05	8.826–05	1.058–04	1.193–04	1.300–04	1.386–04	1.464–04
1	66	1.583–05	7.898–06	6.231–06	5.632–06	5.348–06	5.183–06	5.086–06
1	67	8.635–06	3.133–06	1.806–06	1.252–06	9.519–07	7.656–07	6.382–07
1	68	9.171–06	8.682–06	8.844–06	9.020–06	9.169–06	9.299–06	9.405–06
1	69	1.405–05	4.383–06	2.516–06	1.806–06	1.436–06	1.208–06	1.051–06
1	70	1.753–05	5.197–06	2.385–06	1.347–06	8.580–07	5.914–07	4.313–07
1	71	8.023–06	3.112–06	1.887–06	1.353–06	1.053–06	8.607–07	7.263–07
1	72	2.003–05	9.024–06	7.336–06	6.902–06	6.784–06	6.773–06	6.804–06
1	73	1.037–05	6.051–06	5.324–06	5.077–06	4.954–06	4.872–06	4.816–06
1	74	7.821–06	2.237–06	1.026–06	5.870–07	3.793–07	2.662–07	1.965–07
1	75	1.641–05	5.590–06	3.414–06	2.551–06	2.084–06	1.785–06	1.574–06
1	76	1.317–04	1.799–04	2.132–04	2.387–04	2.596–04	2.768–04	2.928–04
1	77	3.528–06	1.449–06	9.654–07	7.330–07	5.929–07	4.987–07	4.309–07
1	78	3.254–05	4.014–05	4.326–05	4.462–05	4.526–05	4.556–05	4.579–05
1	79	3.251–06	1.004–06	5.963–07	4.315–07	3.408–07	2.828–07	2.423–07
1	80	7.778–06	7.768–06	8.314–06	8.711–06	8.998–06	9.217–06	9.393–06
1	81	2.464–05	2.958–05	3.187–05	3.316–05	3.399–05	3.458–05	3.500–05
1	82	2.109–05	5.094–06	2.199–06	1.217–06	7.722–07	5.338–07	3.914–07
1	83	1.292–05	4.841–06	3.181–06	2.487–06	2.090–06	1.824–06	1.629–06
1	84	8.325–06	2.729–06	1.960–06	1.770–06	1.713–06	1.701–06	1.704–06
1	85	1.768–05	4.513–06	2.017–06	1.152–06	7.549–07	5.399–07	4.100–07
1	86	1.864–05	1.063–05	1.003–05	1.037–05	1.089–05	1.141–05	1.195–05
1	87	5.418–06	1.403–06	6.180–07	3.435–07	2.175–07	1.498–07	1.093–07
1	88	2.929–06	1.389–06	9.772–07	7.621–07	6.262–07	5.320–07	4.630–07
1	89	2.848–06	1.821–06	1.785–06	1.818–06	1.855–06	1.888–06	1.917–06
1	90	9.820–05	1.048–04	1.091–04	1.119–04	1.141–04	1.158–04	1.173–04
1	91	3.847–06	8.577–07	3.809–07	2.160–07	1.392–07	9.709–08	7.153–08

Table 10: Collision strengths for the resonance transitions of Cl XIV. ($a \pm b \equiv a \times 10^{\pm b}$).

Transition		Energy (Ryd)						
<i>i</i>	<i>j</i>	100	200	300	400	500	600	700
1	92	4.113–06	1.078–06	5.710–07	3.861–07	2.925–07	2.360–07	1.983–07
1	93	2.183–05	2.912–05	3.311–05	3.552–05	3.700–05	3.802–05	3.883–05
1	94	1.830–05	2.121–05	2.312–05	2.435–05	2.520–05	2.584–05	2.635–05
1	95	2.100–06	4.082–07	1.587–07	8.248–08	5.014–08	3.360–08	2.405–08
1	96	5.752–05	8.130–05	9.300–05	9.990–05	1.041–04	1.070–04	1.093–04
1	97	6.336–05	6.949–05	7.357–05	7.649–05	7.871–05	8.053–05	8.207–05
1	98	9.632–04	1.357–03	1.615–03	1.811–03	1.971–03	2.103–03	2.226–03

Table 11: Collision strengths for the resonance transitions of K XVI. ($a \pm b \equiv a \times 10^{\pm b}$).

Transition		Energy (Ryd)							
<i>i</i>	<i>j</i>	100	200	300	400	500	600	700	800
1	2	7.875–04	3.346–04	1.837–04	1.160–04	7.985–05	5.847–05	4.455–05	3.512–05
1	3	5.760–03	4.449–03	3.784–03	3.568–03	3.410–03	3.177–03	3.142–03	3.018–03
1	4	3.874–03	1.641–03	8.995–04	5.674–04	3.904–04	2.858–04	2.177–04	1.716–04
1	5	9.055–01	1.050–00	1.013–00	1.046–00	1.034–00	9.672–01	9.974–01	9.398–01
1	6	5.350–05	3.677–05	3.175–05	2.960–05	2.849–05	2.782–05	2.741–05	2.718–05
1	7	5.856–05	1.843–05	8.047–06	4.234–06	2.502–06	1.603–06	1.091–06	7.807–07
1	8	2.891–04	2.489–04	2.432–04	2.432–04	2.445–04	2.462–04	2.482–04	2.487–04
1	9	3.475–03	3.768–03	3.918–03	4.006–03	4.066–03	4.114–03	4.157–03	4.174–03
1	10	1.390–03	1.229–03	1.147–03	1.098–03	1.067–03	1.045–03	1.029–03	1.019–03
1	11	6.855–04	2.406–04	1.230–04	7.478–05	5.033–05	3.631–05	2.737–05	2.148–05
1	12	2.925–02	3.206–02	3.314–02	3.377–02	3.421–02	3.456–02	3.486–02	3.513–02
1	13	2.093–02	3.711–02	4.852–02	5.730–02	6.452–02	7.021–02	7.611–02	8.007–02
1	14	1.918–04	5.812–05	2.715–05	1.558–05	1.003–05	6.985–06	5.133–06	3.934–06
1	15	1.552–02	2.745–02	3.592–02	4.245–02	4.783–02	5.206–02	5.642–02	5.939–02
1	16	9.475–04	2.870–04	1.340–04	7.685–05	4.947–05	3.444–05	2.531–05	1.939–05
1	17	1.031–03	3.167–04	1.496–04	8.637–05	5.598–05	3.914–05	2.885–05	2.214–05
1	18	1.748–03	5.678–04	2.938–04	1.909–04	1.419–04	1.149–04	9.867–05	8.777–05
1	19	2.407–03	7.394–04	3.493–04	2.016–04	1.307–04	9.136–05	6.735–05	5.167–05
1	20	5.342–02	7.163–02	7.968–02	8.422–02	8.708–02	8.904–02	9.066–02	9.122–02
1	21	3.203–06	1.069–06	5.144–07	2.977–07	1.929–07	1.347–07	9.876–08	7.545–08
1	22	1.874–04	3.218–04	4.200–04	4.965–04	5.596–04	6.098–04	6.628–04	6.966–04
1	23	1.476–05	4.958–06	2.391–06	1.386–06	8.998–07	6.293–07	4.623–07	3.539–07
1	24	1.452–03	2.568–03	3.369–03	3.990–03	4.501–03	4.909–03	5.341–03	5.609–03
1	25	3.646–05	1.624–05	9.976–06	7.062–06	5.404–06	4.345–06	3.613–06	3.082–06
1	26	3.056–05	1.399–05	8.772–06	6.300–06	4.871–06	3.947–06	3.302–06	2.829–06
1	27	7.439–05	4.211–05	3.417–05	3.135–05	3.012–05	2.954–05	2.927–05	2.906–05
1	28	7.242–05	2.553–05	1.258–05	7.381–06	4.811–06	3.371–06	2.485–06	1.906–06
1	29	8.536–06	5.882–06	5.334–06	5.165–06	5.104–06	5.083–06	5.081–06	5.088–06
1	30	2.029–05	7.899–06	4.415–06	2.933–06	2.145–06	1.666–06	1.350–06	1.125–06
1	31	3.821–05	1.340–05	8.226–06	6.203–06	5.118–06	4.427–06	3.938–06	3.567–06
1	32	1.264–05	3.817–06	1.717–06	9.525–07	5.986–07	4.078–07	2.954–07	2.227–07
1	33	5.418–05	5.664–05	5.999–05	6.223–05	6.371–05	6.476–05	6.561–05	6.606–05
1	34	5.417–05	2.180–05	1.563–05	1.366–05	1.287–05	1.252–05	1.237–05	1.230–05
1	35	3.978–05	2.095–05	1.667–05	1.450–05	1.301–05	1.186–05	1.093–05	1.016–05
1	36	5.675–05	1.523–05	6.773–06	3.796–06	2.424–06	1.682–06	1.236–06	9.477–07
1	37	3.853–04	5.156–04	5.698–04	5.980–04	6.146–04	6.256–04	6.340–04	6.386–04
1	38	2.097–04	2.854–04	3.396–04	3.814–04	4.155–04	4.432–04	4.721–04	4.899–04
1	39	2.885–05	9.423–06	5.385–06	3.860–06	3.080–06	2.604–06	2.279–06	2.041–06
1	40	1.986–05	9.124–06	7.641–06	7.350–06	7.325–06	7.374–06	7.451–06	7.521–06
1	41	5.305–05	1.559–05	7.336–06	4.290–06	2.842–06	2.042–06	1.553–06	1.232–06
1	42	5.414–05	3.532–05	3.430–05	3.578–05	3.772–05	3.955–05	4.172–05	4.299–05
1	43	1.371–05	4.037–06	1.873–06	1.070–06	6.900–07	4.809–07	3.539–07	2.715–07
1	44	1.313–04	1.283–04	1.280–04	1.282–04	1.285–04	1.289–04	1.294–04	1.299–04
1	45	3.029–04	3.540–04	3.771–04	3.916–04	4.021–04	4.105–04	4.178–04	4.234–04
1	46	2.772–03	3.952–03	4.735–03	5.330–03	5.814–03	6.207–03	6.617–03	6.862–03

Table 11: Collision strengths for the resonance transitions of K XVI. ($a \pm b \equiv a \times 10^{\pm b}$).

Transition		Energy (Ryd)							
<i>i</i>	<i>j</i>	100	200	300	400	500	600	700	800
1	47	2.794–04	8.932–05	4.404–05	2.622–05	1.739–05	1.248–05	9.321–06	7.285–06
1	48	5.580–03	6.304–03	6.594–03	6.755–03	6.864–03	6.950–03	7.020–03	7.084–03
1	49	9.241–05	2.516–05	1.120–05	6.244–06	3.946–06	2.716–06	1.973–06	1.502–06
1	50	8.120–04	1.073–03	1.343–03	1.566–03	1.752–03	1.911–03	2.061–03	2.162–03
1	51	4.569–04	1.243–04	5.529–05	3.082–05	1.947–05	1.340–05	9.730–06	7.403–06
1	52	6.654–03	1.209–02	1.586–02	1.875–02	2.111–02	2.310–02	2.497–02	2.622–02
1	53	4.101–04	1.200–04	5.573–05	3.188–05	2.055–05	1.432–05	1.052–05	8.057–06
1	54	6.907–04	2.112–04	1.058–04	6.692–05	4.859–05	3.857–05	3.254–05	2.865–05
1	55	9.547–04	2.791–04	1.296–04	7.413–05	4.778–05	3.328–05	2.446–05	1.872–05
1	56	8.453–03	1.171–02	1.314–02	1.393–02	1.444–02	1.479–02	1.507–02	1.527–02
1	57	2.293–04	5.015–05	2.035–05	1.081–05	6.665–06	4.510–06	3.252–06	2.456–06
1	58	3.306–04	8.451–05	4.407–05	3.128–05	2.579–05	2.299–05	2.141–05	2.039–05
1	59	4.116–04	8.988–05	3.645–05	1.936–05	1.193–05	8.074–06	5.822–06	4.396–06
1	60	3.194–03	4.231–03	4.537–03	4.674–03	4.755–03	4.809–03	4.858–03	4.883–03
1	61	1.517–06	4.656–07	2.184–07	1.249–07	8.029–08	5.595–08	4.098–08	3.137–08
1	62	1.775–05	2.167–05	2.587–05	2.934–05	3.221–05	3.464–05	3.689–05	3.844–05
1	63	1.009–05	3.584–06	1.957–06	1.295–06	9.503–07	7.440–07	6.082–07	5.129–07
1	64	7.171–06	2.259–06	1.073–06	6.182–07	4.001–07	2.803–07	2.065–07	1.587–07
1	65	4.194–05	5.730–05	6.961–05	7.923–05	8.705–05	9.359–05	9.962–05	1.038–04
1	66	9.225–06	3.126–06	1.670–06	1.093–06	7.978–07	6.220–07	5.077–07	4.270–07
1	67	1.659–05	8.354–06	6.653–06	6.081–06	5.832–06	5.711–06	5.634–06	5.592–06
1	68	1.098–05	1.040–05	1.059–05	1.081–05	1.100–05	1.116–05	1.130–05	1.143–05
1	69	1.673–05	4.780–06	2.467–06	1.638–06	1.235–06	1.002–06	8.499–07	7.426–07
1	70	7.851–06	3.050–06	1.851–06	1.334–06	1.045–06	8.599–07	7.310–07	6.354–07
1	71	2.303–05	1.031–05	8.355–06	7.885–06	7.786–06	7.805–06	7.868–06	7.947–06
1	72	1.895–05	6.004–06	2.830–06	1.620–06	1.040–06	7.201–07	5.264–07	4.013–07
1	73	1.998–05	5.846–06	3.047–06	2.033–06	1.538–06	1.251–06	1.063–06	9.313–07
1	74	1.156–05	7.392–06	6.829–06	6.708–06	6.671–06	6.661–06	6.647–06	6.642–06
1	75	1.316–04	1.827–04	2.182–04	2.455–04	2.679–04	2.869–04	3.041–04	3.173–04
1	76	8.839–06	2.738–06	1.299–06	7.572–07	4.965–07	3.508–07	2.629–07	2.040–07
1	77	3.988–06	1.238–06	7.458–07	5.426–07	4.294–07	3.563–07	3.052–07	2.673–07
1	78	4.953–06	1.239–06	6.397–07	4.292–07	3.249–07	2.627–07	2.213–07	1.917–07
1	79	1.970–05	2.816–05	3.295–05	3.585–05	3.777–05	3.908–05	4.016–05	4.082–05
1	80	7.333–06	6.567–06	7.025–06	7.414–06	7.710–06	7.939–06	8.124–06	8.277–06
1	81	2.029–05	2.301–05	2.465–05	2.544–05	2.584–05	2.609–05	2.618–05	2.626–05
1	82	2.519–05	6.323–06	2.742–06	1.515–06	9.588–07	6.615–07	4.841–07	3.698–07
1	83	1.370–05	4.709–06	2.916–06	2.222–06	1.849–06	1.609–06	1.437–06	1.306–06
1	84	1.077–05	3.237–06	2.072–06	1.755–06	1.648–06	1.610–06	1.600–06	1.602–06
1	85	1.998–05	5.282–06	2.363–06	1.341–06	8.714–07	6.177–07	4.650–07	3.660–07
1	86	1.934–05	9.814–06	8.651–06	8.697–06	9.021–06	9.415–06	9.826–06	1.017–05
1	87	6.314–06	1.714–06	7.670–07	4.291–07	2.726–07	1.880–07	1.373–07	1.046–07
1	88	3.038–06	1.201–06	8.212–07	6.398–07	5.278–07	4.505–07	3.936–07	3.499–07
1	89	6.914–05	7.330–05	7.639–05	7.854–05	8.019–05	8.147–05	8.260–05	8.355–05
1	90	2.847–06	1.262–06	1.126–06	1.120–06	1.135–06	1.153–06	1.171–06	1.187–06
1	91	5.241–06	1.272–06	6.314–07	4.110–07	3.045–07	2.424–07	2.019–07	1.734–07

Table 11: Collision strengths for the resonance transitions of K XVI. ($a \pm b \equiv a \times 10^{\pm b}$).

Transition		Energy (Ryd)							
<i>i</i>	<i>j</i>	100	200	300	400	500	600	700	800
1	92	5.094–06	1.081–06	4.724–07	2.672–07	1.723–07	1.204–07	8.886–08	6.824–08
1	93	1.562–05	2.113–05	2.466–05	2.688–05	2.838–05	2.943–05	3.032–05	3.086–05
1	94	1.272–05	1.441–05	1.590–05	1.692–05	1.765–05	1.821–05	1.865–05	1.901–05
1	95	3.013–06	6.025–07	2.343–07	1.211–07	7.326–08	4.886–08	3.485–08	2.607–08
1	96	3.855–05	5.779–05	6.815–05	7.447–05	7.872–05	8.164–05	8.412–05	8.558–05
1	97	3.947–05	4.424–05	4.774–05	5.020–05	5.207–05	5.356–05	5.482–05	5.589–05
1	98	6.016–04	8.693–04	1.044–03	1.177–03	1.285–03	1.378–03	1.460–03	1.525–03

Table 12: Collision strengths for the resonance transitions of Ge XXIX. ($a \pm b \equiv a \times 10^{\pm b}$).

Transition		Energy (Ryd)							
<i>i</i>	<i>j</i>	500	800	1100	1400	1700	2000	2300	2600
1	2	1.385–04	7.256–05	4.465–05	3.024–05	2.186–05	1.656–05	1.294–05	1.041–05
1	3	2.238–02	1.918–02	1.946–02	1.889–02	1.928–02	1.954–02	1.912–02	1.803–02
1	4	6.449–04	3.358–04	2.059–04	1.390–04	1.003–04	7.589–05	5.924–05	4.761–05
1	5	3.741–01	3.215–01	3.278–01	3.188–01	3.408–01	3.478–01	3.459–01	3.045–01
1	6	9.350–05	8.912–05	8.749–05	8.697–05	8.698–05	8.743–05	8.801–05	8.883–05
1	7	8.877–06	3.896–06	2.093–06	1.278–06	8.490–07	5.981–07	4.425–07	3.389–07
1	8	4.254–04	4.513–04	4.681–04	4.817–04	4.955–04	5.017–04	5.163–04	5.216–04
1	9	3.637–04	3.859–04	4.007–04	4.123–04	4.237–04	4.291–04	4.413–04	4.464–04
1	10	2.018–04	1.911–04	1.860–04	1.835–04	1.823–04	1.823–04	1.827–04	1.838–04
1	11	1.120–04	5.278–05	3.087–05	2.028–05	1.440–05	1.080–05	8.315–06	6.708–06
1	12	1.066–02	1.123–02	1.158–02	1.185–02	1.209–02	1.232–02	1.253–02	1.275–02
1	13	2.949–05	1.264–05	6.885–06	4.317–06	2.948–06	2.129–06	1.608–06	1.261–06
1	14	7.165–03	9.923–03	1.204–02	1.374–02	1.544–02	1.675–02	1.809–02	1.869–02
1	15	1.250–02	1.752–02	2.135–02	2.445–02	2.750–02	2.988–02	3.233–02	3.333–02
1	16	1.419–04	6.063–05	3.298–05	2.065–05	1.408–05	1.016–05	7.663–06	5.999–06
1	17	1.552–04	6.733–05	3.720–05	2.348–05	1.613–05	1.174–05	8.918–06	7.004–06
1	18	6.433–04	5.600–04	5.457–04	5.476–04	5.551–04	5.595–04	5.759–04	5.787–04
1	19	3.645–04	1.580–04	8.729–05	5.508–05	3.781–05	2.753–05	2.090–05	1.641–05
1	20	2.290–02	2.659–02	2.870–02	3.017–02	3.133–02	3.203–02	3.328–02	3.365–02
1	21	4.519–07	2.039–07	1.144–07	7.218–08	4.960–08	3.628–08	2.737–08	2.146–08
1	22	7.275–04	1.012–03	1.230–03	1.406–03	1.578–03	1.711–03	1.857–03	1.906–03
1	23	7.283–06	3.483–06	2.064–06	1.386–06	1.007–06	7.741–07	6.188–07	5.116–07
1	24	7.909–06	7.752–06	7.784–06	7.869–06	7.966–06	8.082–06	8.188–06	8.310–06
1	25	3.193–06	1.545–06	9.353–07	6.432–07	4.789–07	3.763–07	3.078–07	2.591–07
1	26	8.116–05	9.038–05	9.638–05	1.008–04	1.043–04	1.068–04	1.101–04	1.118–04
1	27	1.919–06	8.892–07	5.153–07	3.382–07	2.418–07	1.837–07	1.450–07	1.186–07
1	28	4.704–06	2.121–06	1.301–06	9.354–07	7.371–07	6.153–07	5.335–07	4.751–07
1	29	3.933–04	5.442–04	6.604–04	7.548–04	8.455–04	9.155–04	9.978–04	1.019–03
1	30	2.548–05	2.579–05	2.673–05	2.766–05	2.854–05	2.930–05	3.010–05	3.074–05
1	31	6.415–06	2.915–06	1.764–06	1.243–06	9.607–07	7.872–07	6.720–07	5.906–07
1	32	4.391–04	5.442–04	6.241–04	6.889–04	7.503–04	7.986–04	8.540–04	8.722–04
1	33	1.403–06	7.856–07	5.415–07	4.146–07	3.372–07	2.852–07	2.477–07	2.198–07
1	34	4.477–05	5.146–05	5.533–05	5.800–05	6.007–05	6.156–05	6.335–05	6.435–05
1	35	5.437–06	2.481–06	1.393–06	8.843–07	6.080–07	4.425–07	3.350–07	2.630–07
1	36	1.970–06	1.125–06	7.715–07	5.844–07	4.693–07	3.921–07	3.372–07	2.961–07
1	37	4.325–05	5.028–05	5.421–05	5.685–05	5.886–05	6.034–05	6.198–05	6.298–05
1	38	2.374–06	1.593–06	1.324–06	1.178–06	1.079–06	1.004–06	9.447–07	8.956–07
1	39	3.829–06	1.547–06	8.241–07	5.103–07	3.469–07	2.513–07	1.904–07	1.494–07
1	40	6.444–06	6.220–06	6.364–06	6.552–06	6.747–06	6.918–06	7.103–06	7.247–06
1	41	1.329–05	1.455–05	1.610–05	1.753–05	1.896–05	2.009–05	2.147–05	2.189–05
1	42	1.071–06	4.574–07	2.507–07	1.575–07	1.080–07	7.850–08	5.962–08	4.683–08
1	43	1.747–05	1.759–05	1.780–05	1.805–05	1.829–05	1.856–05	1.880–05	1.908–05
1	44	3.537–06	1.581–06	9.320–07	6.382–07	4.796–07	3.831–07	3.197–07	2.755–07
1	45	4.489–05	4.989–05	5.307–05	5.545–05	5.750–05	5.917–05	6.089–05	6.219–05
1	46	5.784–04	7.200–04	8.275–04	9.148–04	9.968–04	1.060–03	1.136–03	1.160–03

Table 12: Collision strengths for the resonance transitions of Ge XXIX. ($a \pm b \equiv a \times 10^{\pm b}$).

Transition		Energy (Ryd)							
<i>i</i>	<i>j</i>	500	800	1100	1400	1700	2000	2300	2600
1	47	4.423–05	1.984–05	1.134–05	7.334–06	5.165–06	3.844–06	2.954–06	2.361–06
1	48	2.056–03	2.198–03	2.281–03	2.344–03	2.397–03	2.446–03	2.491–03	2.535–03
1	49	1.332–05	5.396–06	2.852–06	1.748–06	1.178–06	8.400–07	6.316–07	4.899–07
1	50	1.038–03	1.429–03	1.733–03	1.984–03	2.204–03	2.377–03	2.585–03	2.689–03
1	51	6.420–05	2.593–05	1.367–05	8.363–06	5.625–06	4.006–06	3.007–06	2.330–06
1	52	2.911–03	4.117–03	5.036–03	5.792–03	6.450–03	6.967–03	7.587–03	7.899–03
1	53	5.989–05	2.535–05	1.385–05	8.676–06	5.933–06	4.303–06	3.260–06	2.554–06
1	54	1.967–04	1.591–04	1.509–04	1.495–04	1.505–04	1.522–04	1.543–04	1.565–04
1	55	1.387–04	5.858–05	3.198–05	2.002–05	1.369–05	9.922–06	7.516–06	5.886–06
1	56	3.328–03	3.930–03	4.273–03	4.506–03	4.685–03	4.829–03	4.956–03	5.067–03
1	57	3.001–05	1.074–05	5.360–06	3.185–06	2.102–06	1.490–06	1.111–06	8.597–07
1	58	1.694–04	1.620–04	1.632–04	1.656–04	1.683–04	1.707–04	1.743–04	1.761–04
1	59	5.335–05	1.905–05	9.492–06	5.635–06	3.718–06	2.635–06	1.963–06	1.520–06
1	60	1.340–03	1.511–03	1.592–03	1.644–03	1.685–03	1.717–03	1.758–03	1.779–03
1	61	2.101–07	9.089–08	5.009–08	3.147–08	2.158–08	1.572–08	1.183–08	9.311–09
1	62	1.255–05	1.602–05	1.875–05	2.101–05	2.299–05	2.456–05	2.643–05	2.741–05
1	63	1.508–06	6.774–07	3.896–07	2.578–07	1.860–07	1.426–07	1.142–07	9.452–08
1	64	9.379–06	9.782–06	1.010–05	1.037–05	1.061–05	1.083–05	1.105–05	1.125–05
1	65	1.264–06	5.528–07	3.115–07	2.031–07	1.442–07	1.088–07	8.607–08	7.028–08
1	66	3.394–06	3.043–06	3.086–06	3.187–06	3.291–06	3.389–06	3.477–06	3.558–06
1	67	2.173–06	8.792–07	4.879–07	3.207–07	2.337–07	1.823–07	1.492–07	1.263–07
1	68	3.156–06	1.289–06	7.038–07	4.492–07	3.164–07	2.382–07	1.882–07	1.542–07
1	69	5.636–06	5.385–06	5.603–06	5.861–06	6.104–06	6.329–06	6.535–06	6.728–06
1	70	1.183–04	1.475–04	1.695–04	1.876–04	2.033–04	2.162–04	2.305–04	2.398–04
1	71	4.581–07	1.923–07	1.143–07	7.962–08	6.068–08	4.896–08	4.109–08	3.548–08
1	72	1.843–05	2.318–05	2.609–05	2.808–05	2.970–05	3.083–05	3.195–05	3.266–05
1	73	8.313–07	3.061–07	1.622–07	1.034–07	7.355–08	5.620–08	4.515–08	3.760–08
1	74	2.552–06	2.806–06	3.039–06	3.222–06	3.372–06	3.497–06	3.610–06	3.708–06
1	75	4.198–07	1.788–07	9.724–08	6.052–08	4.125–08	2.996–08	2.252–08	1.774–08
1	76	7.840–06	9.866–06	1.146–05	1.277–05	1.391–05	1.483–05	1.591–05	1.649–05
1	77	5.099–07	2.483–07	1.576–07	1.149–07	9.036–08	7.470–08	6.397–08	5.611–08
1	78	1.576–06	1.429–06	1.425–06	1.444–06	1.468–06	1.492–06	1.514–06	1.536–06
1	79	1.463–06	6.261–07	3.400–07	2.114–07	1.432–07	1.032–07	7.759–08	6.046–08
1	80	8.202–07	4.177–07	2.685–07	1.956–07	1.527–07	1.251–07	1.061–07	9.213–08
1	81	1.887–06	2.052–06	2.186–06	2.282–06	2.355–06	2.415–06	2.465–06	2.509–06
1	82	7.756–07	3.967–07	2.820–07	2.297–07	1.995–07	1.794–07	1.649–07	1.537–07
1	83	1.690–06	6.578–07	3.440–07	2.108–07	1.422–07	1.025–07	7.741–08	6.052–08
1	84	1.295–06	9.103–07	8.394–07	8.331–07	8.454–07	8.640–07	8.844–07	9.054–07
1	85	1.102–05	1.164–05	1.207–05	1.242–05	1.273–05	1.301–05	1.328–05	1.353–05
1	86	3.402–06	3.395–06	3.652–06	3.937–06	4.214–06	4.454–06	4.727–06	4.916–06
1	87	4.653–07	1.894–07	1.012–07	6.252–08	4.234–08	3.053–08	2.303–08	1.799–08
1	88	1.419–06	5.832–07	3.232–07	2.103–07	1.514–07	1.166–07	9.428–08	7.899–08
1	89	2.007–07	1.131–07	8.342–08	6.778–08	5.785–08	5.087–08	4.567–08	4.163–08
1	90	1.392–07	5.069–08	2.809–08	1.922–08	1.488–08	1.246–08	1.101–08	1.008–08
1	91	3.369–06	4.162–06	4.672–06	5.030–06	5.324–06	5.526–06	5.733–06	5.851–06

Table 12: Collision strengths for the resonance transitions of Ge XXIX. ($a \pm b \equiv a \times 10^{\pm b}$).

Transition		Energy (Ryd)							
<i>i</i>	<i>j</i>	500	800	1100	1400	1700	2000	2300	2600
1	92	3.515–07	1.520–07	9.455–08	6.922–08	5.526–08	4.645–08	4.040–08	3.597–08
1	93	4.735–06	5.445–06	5.960–06	6.355–06	6.678–06	6.957–06	7.203–06	7.429–06
1	94	3.106–07	1.184–07	6.304–08	3.930–08	2.688–08	1.955–08	1.485–08	1.166–08
1	95	2.315–06	2.661–06	2.907–06	3.092–06	3.241–06	3.364–06	3.474–06	3.571–06
1	96	2.216–07	7.625–08	3.718–08	2.173–08	1.418–08	9.959–09	7.370–09	5.668–09
1	97	1.143–04	1.430–04	1.647–04	1.825–04	1.979–04	2.107–04	2.248–04	2.343–04
1	98	1.087–05	1.372–05	1.547–05	1.668–05	1.767–05	1.834–05	1.904–05	1.943–05

Table 16: Comparisons of effective collision strengths for transitions among the lowest 10 levels of Cl XIV.
 $a \pm b \equiv a \times 10^{\pm b}$.

Transition		RM ($\log T_e$, K)			DARC ($\log T_e$, K)			Ratio R ($\log T_e$, K)		
I	J	6.30	6.50	6.70	6.30	6.50	6.70	6.30	6.50	6.70
1	2	3.605–3	3.104–3	2.610–3	5.797–3	5.271–3	4.459–3	1.61	1.70	1.71
1	3	1.237–2	1.096–2	9.588–3	1.901–2	1.750–2	1.511–2	1.54	1.60	1.58
1	4	1.815–2	1.556–2	1.304–2	2.978–2	2.711–2	2.292–2	1.64	1.74	1.76
1	5	8.039–1	8.567–1	9.185–1	7.984–1	8.391–1	8.922–1	0.99	0.98	0.97
1	6	1.292–4	1.134–4	9.763–5	4.055–4	4.057–4	3.582–4	3.14	3.58	3.67
1	7	3.152–4	2.715–4	2.273–4	9.447–4	9.212–4	7.970–4	3.00	3.39	3.51
1	8	6.011–4	5.273–4	4.556–4	1.582–3	1.541–3	1.349–3	2.63	2.92	2.96
1	9	4.303–3	4.318–3	4.365–3	6.544–3	6.488–3	6.263–3	1.52	1.50	1.43
1	10	2.214–3	2.152–3	2.080–3	3.403–3	3.341–3	3.112–3	1.54	1.55	1.50
2	3	5.997–2	4.759–2	3.719–2	6.190–2	5.271–2	4.289–2	1.03	1.11	1.15
2	4	4.578–2	3.761–2	3.152–2	4.747–2	4.252–2	3.727–2	1.04	1.13	1.18
2	5	9.023–3	7.523–3	6.168–3	1.636–2	1.496–2	1.254–2	1.81	1.99	2.03
2	6	2.270–3	1.965–3	1.662–3	3.194–3	2.935–3	2.504–3	1.41	1.49	1.51
2	7	3.976–1	4.255–1	4.572–1	3.886–1	4.058–1	4.239–1	0.98	0.95	0.93
2	8	3.195–3	2.849–3	2.474–3	7.511–3	6.984–3	5.934–3	2.35	2.45	2.40
2	9	3.797–3	3.367–3	2.903–3	8.337–3	7.759–3	6.574–3	2.20	2.30	2.26
2	10	4.772–4	4.228–4	3.637–4	1.276–3	1.153–3	9.500–4	2.67	2.73	2.61
3	4	2.068–1	1.626–1	1.289–1	2.090–1	1.776–1	1.477–1	1.01	1.09	1.15
3	5	2.757–2	2.298–2	1.886–2	5.088–2	4.603–2	3.836–2	1.85	2.00	2.03
3	6	3.938–1	4.233–1	4.564–1	3.926–1	4.090–1	4.232–1	1.00	0.97	0.93
3	7	3.038–1	3.242–1	3.470–1	3.059–1	3.176–1	3.280–1	1.01	0.98	0.95
3	8	5.030–1	5.358–1	5.729–1	5.005–1	5.211–1	5.414–1	1.00	0.97	0.95
3	9	1.476–2	1.354–2	1.225–2	2.925–2	2.727–2	2.342–2	1.98	2.01	1.91
3	10	1.759–3	1.602–3	1.430–3	4.518–3	4.126–3	3.443–3	2.57	2.58	2.41
4	5	4.959–2	4.069–2	3.292–2	8.871–2	7.870–2	6.482–2	1.79	1.93	1.97
4	6	2.864–3	2.443–3	2.049–3	5.409–3	5.013–3	4.249–3	1.89	2.05	2.07
4	7	4.970–1	5.322–1	5.709–1	5.110–1	5.351–1	5.574–1	1.03	1.01	0.98
4	8	1.463–0	1.567–0	1.683–0	1.459–0	1.524–0	1.587–0	1.00	0.97	0.94
4	9	4.631–2	4.398–2	4.110–2	8.777–2	8.505–2	7.871–2	1.90	1.93	1.92
4	10	3.153–3	2.797–3	2.412–3	9.261–3	8.432–3	6.983–3	2.94	3.01	2.90
5	6	4.650–3	4.263–3	3.863–3	8.836–3	8.243–3	7.313–3	1.90	1.93	1.89
5	7	1.021–2	8.885–3	7.590–3	2.060–2	1.863–2	1.568–2	2.02	2.10	2.07
5	8	3.504–2	3.298–2	3.054–2	7.028–2	6.751–2	6.334–2	2.01	2.05	2.07
5	9	2.034–0	2.182–0	2.339–0	2.068–0	2.140–0	2.211–0	1.02	0.98	0.95
5	10	6.986–1	7.484–1	8.037–1	6.886–1	7.193–1	7.455–1	0.99	0.96	0.93
6	7	3.387–2	3.015–2	2.615–2	5.524–2	5.075–2	4.318–2	1.63	1.68	1.65
6	8	2.573–2	2.511–2	2.451–2	3.803–2	3.666–2	3.381–2	1.48	1.46	1.38
6	9	1.656–2	1.462–2	1.256–2	2.555–2	2.350–2	1.989–2	1.54	1.61	1.58
6	10	1.977–3	1.693–3	1.404–3	6.218–3	5.578–3	4.546–3	3.15	3.29	3.24
7	8	9.747–2	9.208–2	8.670–2	1.543–1	1.458–1	1.297–1	1.58	1.58	1.50
7	9	5.545–2	4.915–2	4.242–2	8.816–2	8.134–2	6.908–2	1.59	1.65	1.63
7	10	6.520–3	5.583–3	4.630–3	1.929–2	1.728–2	1.408–2	2.96	3.10	3.04
8	9	1.028–1	9.183–2	7.993–2	1.691–1	1.557–1	1.325–1	1.64	1.70	1.66
8	10	1.169–2	1.013–2	8.524–3	3.056–2	2.745–2	2.255–2	2.61	2.71	2.65
9	10	5.278–2	5.404–2	5.577–2	6.842–2	6.862–2	6.790–2	1.30	1.27	1.22

Table 17: Comparisons of effective collision strengths for transitions among the lowest 10 levels of K XVI.
 $a \pm b \equiv a \times 10^{\pm b}$.

Transition		RM ($\log T_e$, K)			DARC ($\log T_e$, K)			Ratio R ($\log T_e$, K)		
I	J	6.50	6.70	6.90	6.50	6.70	6.90	6.50	6.70	6.90
1	2	2.475–3	2.134–3	1.788–3	4.566–3	3.973–3	3.241–3	1.84	1.86	1.81
1	3	9.706–3	8.872–3	8.079–3	1.625–2	1.458–2	1.251–2	1.67	1.64	1.55
1	4	1.253–2	1.072–2	8.919–3	2.484–2	2.132–2	1.722–2	1.98	1.99	1.93
1	5	6.596–1	7.096–1	7.664–1	6.621–1	7.043–1	7.614–1	1.00	0.99	0.99
1	6	1.178–4	1.034–4	8.983–5	3.380–4	3.166–4	2.684–4	2.87	3.06	2.99
1	7	2.362–4	1.996–4	1.636–4	7.496–4	6.867–4	5.662–4	3.17	3.44	3.46
1	8	5.110–4	4.489–4	3.934–4	1.260–3	1.175–3	1.008–3	2.47	2.62	2.56
1	9	2.593–3	2.655–3	2.752–3	4.392–3	4.293–3	4.138–3	1.69	1.62	1.50
1	10	1.653–3	1.606–3	1.552–3	2.429–3	2.327–3	2.137–3	1.47	1.45	1.38
2	3	3.763–2	2.991–2	2.344–2	4.873–2	4.008–2	3.162–2	1.29	1.34	1.35
2	4	2.772–2	2.373–2	2.087–2	3.708–2	3.240–2	2.797–2	1.34	1.37	1.34
2	5	6.275–3	5.205–3	4.225–3	1.273–2	1.115–2	9.006–3	2.03	2.14	2.13
2	6	1.812–3	1.515–3	1.241–3	2.610–3	2.337–3	1.940–3	1.44	1.54	1.56
2	7	3.185–1	3.450–1	3.738–1	3.190–1	3.380–1	3.636–1	1.00	0.98	0.97
2	8	2.733–3	2.399–3	2.044–3	6.437–3	5.706–3	4.668–3	2.36	2.38	2.28
2	9	2.248–3	1.968–3	1.671–3	5.810–3	5.165–3	4.216–3	2.58	2.62	2.52
2	10	2.714–4	2.360–4	1.986–4	9.128–4	7.856–4	6.226–4	3.36	3.33	3.13
3	4	1.473–1	1.147–1	9.099–2	1.616–1	1.339–1	1.092–1	1.10	1.17	1.20
3	5	1.949–2	1.617–2	1.316–2	4.007–2	3.467–2	2.788–2	2.06	2.14	2.12
3	6	3.163–1	3.444–1	3.744–1	3.221–1	3.374–1	3.551–1	1.02	0.98	0.95
3	7	2.420–1	2.618–1	2.828–1	2.503–1	2.622–1	2.771–1	1.03	1.00	0.98
3	8	4.042–1	4.359–1	4.700–1	4.114–1	4.334–1	4.627–1	1.02	0.99	0.98
3	9	1.122–2	1.055–2	9.893–3	2.330–2	2.120–2	1.822–2	2.08	2.01	1.84
3	10	1.221–3	1.123–3	1.019–3	3.434–3	3.013–3	2.458–3	2.81	2.68	2.41
4	5	3.728–2	2.999–2	2.373–2	5.595–2	5.039–2	4.146–2	1.50	1.68	1.75
4	6	2.183–3	1.763–3	1.407–3	4.189–3	3.744–3	3.065–3	1.92	2.12	2.18
4	7	3.958–1	4.308–1	4.673–1	4.137–1	4.345–1	4.606–1	1.05	1.01	0.99
4	8	1.142–0	1.239–0	1.342–0	1.159–0	1.221–0	1.301–0	1.01	0.99	0.97
4	9	6.390–2	6.412–2	6.405–2	9.988–2	9.801–2	9.515–2	1.56	1.53	1.49
4	10	2.318–3	2.021–3	1.710–3	7.355–3	6.405–3	5.129–3	3.17	3.17	3.00
5	6	4.859–3	4.684–3	4.521–3	8.519–3	8.044–3	7.395–3	1.75	1.72	1.64
5	7	7.848–3	6.822–3	5.852–3	1.670–2	1.493–2	1.245–2	2.13	2.19	2.13
5	8	5.401–2	5.466–2	5.485–2	8.887–2	8.839–2	8.766–2	1.65	1.62	1.60
5	9	1.562–0	1.703–0	1.845–0	1.806–0	1.918–0	2.018–0	1.16	1.13	1.09
5	10	5.683–1	6.165–1	6.669–1	5.731–1	6.040–1	6.371–1	1.01	0.98	0.96
6	7	2.515–2	2.204–2	1.884–2	4.176–2	3.694–2	3.046–2	1.66	1.68	1.62
6	8	2.105–2	2.036–2	1.969–2	3.051–2	2.862–2	2.601–2	1.45	1.41	1.32
6	9	1.065–2	9.209–3	7.721–3	1.828–2	1.615–2	1.320–2	1.72	1.75	1.71
6	10	1.336–3	1.131–3	9.268–4	5.005–3	4.287–3	3.368–3	3.75	3.79	3.63
7	8	7.483–2	6.977–2	6.491–2	1.192–1	1.088–1	9.456–2	1.59	1.56	1.46
7	9	3.959–2	3.448–2	2.921–2	6.996–2	6.227–2	5.130–2	1.77	1.81	1.76
7	10	4.792–3	4.055–3	3.320–3	1.580–2	1.354–2	1.065–2	3.30	3.34	3.21
8	9	8.090–2	7.148–2	6.153–2	1.401–1	1.244–1	1.034–1	1.73	1.74	1.68
8	10	9.236–3	8.001–3	6.743–3	2.361–2	2.042–2	1.640–2	2.56	2.55	2.43
9	10	4.187–2	4.309–2	4.476–2	5.418–2	5.369–2	5.288–2	1.29	1.25	1.18